ISPRS Journal of Photogrammetry and Remote Sensing 181 (2021) 308–326

Contents lists available at ScienceDirect

ISPRS Journal of Photogrammetry and Remote Sensing

journal homepage: www.elsevier.com/locate/isprsjprs

Hybrid phenology matching model for robust crop phenological retrieval

Chunyuan Diao [a,*], Zijun Yang [a], Feng Gao [b], Xiaoyang Zhang [c], Zhengwei Yang [d]

[a] Department of Geography and Geographic Information Science, University of Illinois at Urbana-Champaign, Urbana, IL 61801, USA
[b] United States Department of Agriculture, Agricultural Research Service, Hydrology and Remote Sensing Laboratory, Beltsville, MD 20705, USA
[c] Department of Geography and Geospatial Sciences, South Dakota State University, Brookings, SD 57007, USA
[d] United States Department of Agriculture, National Agricultural Statistics Service, Research and Development Division, Washington, DC 20250, USA

ARTICLE INFO

Keywords:
Phenology
Remote sensing
Agriculture
Crop progress
Planting date

ABSTRACT

Crop phenology regulates seasonal agroecosystem carbon, water, and energy exchanges, and is a key component in empirical and process-based crop models for simulating biogeochemical cycles of farmlands, assessing gross and net primary production, and forecasting the crop yield. The advances in phenology matching models provide a feasible means to monitor crop phenological progress using remote sensing observations, with a priori information of reference shapes and reference phenological transition dates. Yet the underlying geometrical scaling assumption of models, together with the challenge in defining phenological references, hinders the applicability of phenology matching in crop phenological studies. The objective of this study is to develop a novel hybrid phenology matching model to robustly retrieve a diverse spectrum of crop phenological stages using satellite time series. The devised hybrid model leverages the complementary strengths of phenometric extraction methods and phenology matching models. It relaxes the geometrical scaling assumption and can characterize key phenological stages of crop cycles, ranging from farming practice-relevant stages (e.g., planted and harvested) to crop development stages (e.g., emerged and mature). To systematically evaluate the influence of phenological references on phenology matching, four representative phenological reference scenarios under varying levels of phenological calibrations in terms of time and space are further designed with publicly accessible phenological information. The results indicate that the hybrid phenology matching model can achieve high accuracies for estimating corn and soybean phenological growth stages in Illinois, particularly with the year- and region-adjusted phenological reference (R-squared higher than 0.9 and RMSE less than 5 days for most phenological stages). The inter-annual and regional phenological patterns characterized by the hybrid model correspond well with those in the crop progress reports (CPRs) from the USDA National Agricultural Statistics Service (NASS). Compared to the benchmark phenology matching model, the hybrid model is more robust to the decreasing levels of phenological reference calibrations, and is particularly advantageous in retrieving crop early phenological stages (e.g., planted and emerged stages) when the phenological reference information is limited. This innovative hybrid phenology matching model, together with CPR-enabled phenological reference calibrations, holds considerable promise in revealing spatio-temporal patterns of crop phenology over extended geographical regions.

1. Introduction

The vegetation phenological dynamics regulate intra- and inter-annual biosphere-atmosphere interactions, and are key indicators of climatic and environmental changes in terrestrial ecosystems (Cleland et al., 2007; Richardson et al., 2013; White et al., 2005; Xu et al., 2020). The phenological progress of crops plays an essential role in modeling seasonal agroecosystem carbon, water, and energy exchanges, assessing biomass accumulation and net primary production, and scheduling farm management practices (e.g., irrigation, fertilizer, and other chemical applications) (Chen et al., 2015; Liao et al., 2019; Lokupitiya et al., 2009; Magney et al., 2016; Viña et al., 2004; Walthall et al., 2013). Crop phenology is also a critical parameter in empirical and process-based crop models for yield forecasting and estimation, which has marked implications for food security, commodity trading, and risk management (Bolton and Friedl, 2013; Funk and Budde, 2009; Gao et al., 2018; Johnson, 2014; Sakamoto et al., 2013). As the sensitivity of crop growth to climate change and weather anomalies (e.g., water and heat stress)

* Corresponding author.
E-mail address: chunyuan@illinois.edu (C. Diao).

https://doi.org/10.1016/j.isprsjprs.2021.09.011
Received 5 May 2021; Received in revised form 28 July 2021; Accepted 10 September 2021

differs across crop physiological growth stages, such phenological information is crucial to assess the influence of weather stress on yield loss and to support targeted interventions for resilient agricultural development. For instance, water stress has considerably damaging effects on yields particularly during the silking stage of corn, and during the latter part of the reproductive stages of soybean (De Souza et al., 1997; Lauer, 2012; Viña et al., 2004). Affected by a combination of weather conditions, soil properties, landscape variations and anthropogenic activities, crop phenological development trajectories may vary widely across geographic locations and years (Brown and de Beurs, 2008; Brown et al., 2012; Siebert and Ewert, 2012). Accurate monitoring of crop phenology over space and time is imperative to advance farm management practices, and to improve agricultural resilience to adverse environmental conditions.

Remote sensing provides a feasible solution to monitor crop phenological stages over large geographical regions in a repeated and consistent fashion. With the satellite time series, a range of phenological transition dates that are characteristic of crop phenological stages have been explored (Diao, 2019; Gao et al., 2020a; Gao et al., 2020b; Gao et al., 2017; Liu et al., 2018; Wardlow et al., 2006; Zeng et al., 2020). In particular, Diao (2020) developed a remote sensing phenological monitoring framework that comprises three major constituents to detect a multitude of crop phenological stages. Those constituents are time series phenological pre-processing, time series phenological modeling, and time series phenological characterization. Time series phenological pre-processing consists of outlier and seasonality filtering to smooth the satellite time series, to remove spurious observations, and to eliminate the influence of off-season vegetation covers (e.g., weed and cover crop). Time series phenological modeling includes several curve fitting-based phenological models (e.g., three variants of double logistic models and a data-driven spline model) to track the rapid growth of crops throughout the growing season, and to model their seasonal phenological patterns. Time series phenological characterization encompasses diverse phenometric extraction methods (e.g., curve derivative- and curvature-based methods) to estimate the transition dates that denote the timings of crop phenological development shifting from one stage to another. With a systematic set of methodology, the phenological framework embodies comprehensive remote monitoring strategies to detect several corn and soybean growth stages using satellite time series. Despite the promising results, the crop growth stages are mostly characterized in terms of satellite time series curve properties (e.g., inflection points), the potential of which to extend to other physiological growth stages may be limited. Detecting the growth stages that do not maintain distinct curve properties may be challenging. Besides, the crop planting dates, when crops do not produce vegetative remotely sensed signals, cannot be detected using the phenological framework.

As the initial timing of crop growth, crop planting dates represent the time boundary of seasonal carbon, water, and energy exchanges between croplands and atmosphere (Rosenzweig et al., 2013; Twine et al., 2004). The planting dates affect agricultural management practices of subsequent phenological stages, regulate the weather conditions experienced by crops over the growing season, and have considerable controls on crop growth and yields (Kogan et al., 2013; Müller et al., 2019; Ortiz-Monasterio et al., 1994; Otegui et al., 1995). Delayed planting of corn in the Midwestern US may cause large reductions in yield, since the crop is more inclined to encounter water or heat stress during its vegetative and reproductive stages (Irwin et al., 2015). Crop planting dates are also essential parameters in process-based crop simulation models to estimate dry matter accumulation and crop yields (Folberth et al., 2012; Keating et al., 2003; Moulin et al., 1998). At regional to global scales, many crop models assume fixed planting dates (or specified planting time windows), or assume a relationship between planting dates and weather conditions (e.g., temperature and precipitation) (Bondeau et al., 2007; Müller et al., 2019; Sacks et al., 2010). However, crop planting dates are influenced by both environmental conditions (e.g., weather and soil) and farming activities (Kucharik, 2006). Adjusting the planting dates is one of the most critical adaptation strategies to mitigate yield loss in the face of climate change and increasing climatic variability (Lauer et al., 1999; Liu et al., 2013; Nendel et al., 2014; Waha et al., 2013). The complexity of the combined environmental and anthropogenic factors makes the estimation of spatio-temporal patterns of planting dates challenging. To accommodate the spatio-temporal phenological variations, remotely sensed phenological characteristics have been employed to estimate crop planting dates with varying success (Jain et al., 2016; Liu et al., 2018; Manfron et al., 2017; Sadeh et al., 2019; Sakamoto et al., 2005; Son et al., 2016; Urban et al., 2018). Those studies generally assume that the planting dates can be correlated with the greenup onset dates (i.e., start of the growing season) of the satellite time series. The dates of greenup onset can be characterized from the satellite time series by threshold-defined algorithms (e.g., 10% of the amplitude), inflection point algorithms (e.g., local maxima or minima of the rate of curvature change), or moving average algorithms (e.g., change of short and long moving averages) (Gao et al., 2020a; Gao et al., 2020b; White et al., 2009; Zhang et al., 2003). Yet the greenup onset dates have been found to approximate the phenological stage of crop emergence, instead of the planted stage (Gao et al., 2020a; Gao et al., 2017; Ren et al., 2017; Wardlow et al., 2006; Xu et al., 2017). Large timing gaps (e.g., 2–3 weeks) may exist between the satellite detected characteristics and observed planting dates. Despite the relationship assumed between crop planting and emergence dates, the correlation estimated may be subject to local agro-meteorological conditions, and might not be extrapolated over space and time for effective planting date estimation (Abendroth et al., 2011; Kucharik, 2006). A more accurate and robust remotely sensed measure that can be directly characteristic of crop planting dates is to be developed.

Apart from the critical need to retrieve crop planting dates, it is important to develop appropriate modeling strategies that can be flexible in remotely detecting a diverse set of crop growth stages with significant physiological implications. Some key crop growth stages with no distinctive vegetated feature change may be challenging to identify using curve properties (e.g., inflection points) of satellite time series. With a priori information of reference shapes and reference phenological transition dates (a.k.a. reference dates), phenology matching models provide desired alternatives to characterize specific phenological stages along the crop seasonal growth trajectory (Zeng et al., 2020). Reference shapes are crop-specific geometrical patterns that are representative of typical satellite time series profiles of crop growth, and reference dates are pre-defined phenological transition dates on reference shapes based on ground phenological observations. As the prime phenology matching model, the shape model fitting (SMF) method assumes that crop phenological patterns embedded in the satellite time series can be approximated through geometrical scaling of crop-specific reference shapes (i.e., geometrical scaling assumption) (Sakamoto et al., 2013; Sakamoto et al., 2011; Sakamoto et al., 2010; Sun et al., 2021; Zeng et al., 2020). The phenological transition dates can then be estimated using the corresponding optimum scaling parameters, coupled with crop-specific reference dates (Sakamoto et al., 2010). By characterizing macroscopic scaling features, the SMF method can reduce the influence of localized fluctuations in the satellite time series, as well as estimate crop transition dates connected to its physiological growth stages. Despite the potential of the SMF method for crop phenological characterization, the geometrical scaling assumption between reference shapes and crop satellite time series curves might not be satisfied over extended geographical regions, given that a variety of factors might affect the annual crop growth profile. A more robust phenology matching strategy that can relax the shape model assumption is to be explored. Additionally, the performance of the SMF method is influenced by the characteristics of a priori reference shapes and reference dates, which are typically defined based on limited field sites and phenological observations (but see Sakamoto (2018)). The selection of field sites may be opportunistic, and the site-specific crop reference information might not be representative across locations and years. As the theoretical basis for

phenology matching, the reference shapes and dates exert a significant role in determining phenological retrieval accuracy. Thus a systematic evaluation of strategies to design reference shapes and dates, particularly using publicly accessible crop phenological information, is desired.

The objective of this study is to develop a novel hybrid phenology matching model to robustly retrieve a range of crop phenological growth stages using satellite time series. The devised hybrid model leverages the complementary strengths of phenometric extraction and phenology matching models. It relaxes the geometrical scaling assumption and can characterize key phenological stages of crop cycles, ranging from farming practice-relevant stages (e.g., planted and harvested) to crop development stages (e.g., emerged and mature). Specifically, we seek to 1) devise the hybrid phenology matching model for crop phenological characterization; 2) evaluate the performance of the hybrid model under various designs of reference shapes and dates with publicly available phenological information; and 3) compare the devised hybrid model with the benchmark SMF method in estimating a variety of crop phenological stages. The hybrid phenology matching model is assessed for corn and soybean in Illinois from 2002 to 2017.

2. Study site and data

2.1. Study site

The study site is the state of Illinois. Located in the Midwest, Illinois is a leading agricultural production state in the US. With a maximum north-south distance of over 600 km, the climate varies widely throughout the state. The diverse weather and environmental conditions, along with different farm management practices, result in a variety of crop phenological development trajectories across regions and years. Corn and soybean are the two major agricultural crops grown in the state, taking up more than 95% of the croplands. Most fields in Illinois belong to rainfed and monoculture systems, with crop rotation between corn and soybean commonly practiced. The state consists of nine agricultural statistics districts (ASD), and each ASD contains a group of counties that are geographically conterminous with comparable agricultural characteristics (Fig. 1). The nine ASDs are southwest (SW), southeast (SE), west southwest (WSW), east southeast (ESE), west (W), central (C), east (E), northwest (NW), and northeast (NE) ASDs. The large acreage of crops and the variation in crop phenology across the state make Illinois specifically suitable for this study.

2.2. Remote sensing and ground reference data

The Moderate Resolution Imaging Spectroradiometer (MODIS) MCD43A4 nadir Bidirectional Reflectance Distribution Function (BRDF) adjusted reflectance dataset is employed as the main source of remote sensing data to extract satellite time series phenological information of corn and soybean (Schaaf and Wang, 2015). With its daily temporal resolution and 500 m spatial resolution, the MODIS MCD43A4 dataset has been used for vegetation phenological monitoring at regional to global scales. For each date, the surface reflectances during the 16-day period are utilized to build the semi-empirical BRDF model and then to compute Nadir BRDF-adjusted Reflectance (NBAR) to remove view angle effects. The MCD43A4 data covering the study site from 2002 to 2017 are acquired, and the time series of normalized difference vegetation index (NDVI) is derived on a per-pixel basis for crop phenological monitoring. The NDVI time series is pre-processed using the snow/ice quality layer of the MCD43A2 product and the land surface temperature layer of the MOD11A1 product (Wan et al., 2002). These ancillary layers are employed to filter out outlying observations caused by snow or ice contamination. Specifically, the NDVI observations with snow-cover or daytime surface skin temperatures less than 5 °C are flagged as spurious observations, which are then replaced by the mean values of good quality neighboring observations in the time series similar to Zhang et al. (2006). Complementary to the snow/ice quality layer, the 5 °C daytime temperature is utilized to reduce the influence of partial snow, ice, and other background conditions in winter (Zhang and Goldberg, 2011). The NDVI time series is further pre-processed using a combination of outlier filters (e.g., blue, spline, and median filters) to diminish the effects of cloud, snow, and other residual contaminations, as well as the seasonality filter to eliminate the influence of off-season vegetation covers. The pre-processed NDVI time series is then fitted with a double logistic function to generate more consistent and stable crop phenological patterns for subsequent analyses. More information of NDVI time series pre-processing can be found in the previous study (Diao, 2020).

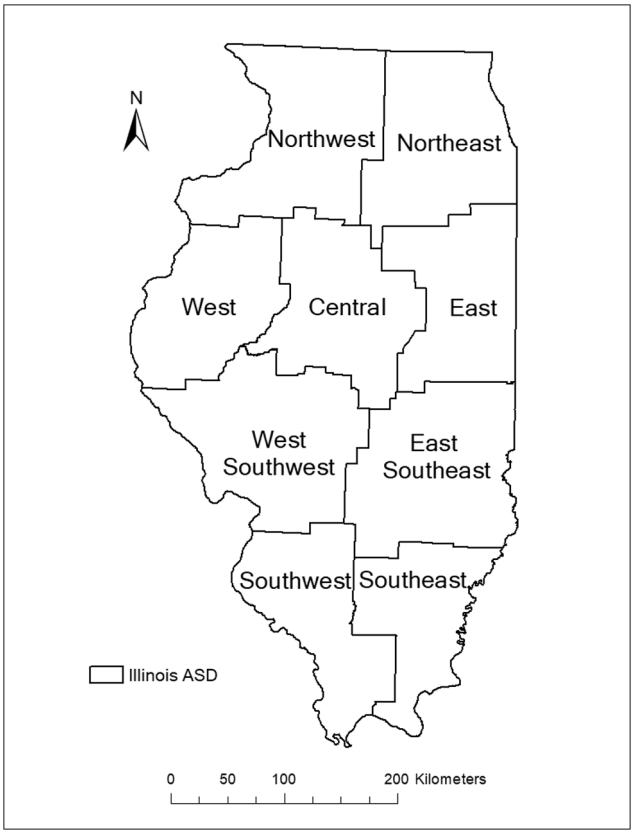

Fig. 1. The nine ASDs in Illinois, US.

With the spatial resolution of 500 m, the phenological information in one MODIS pixel may contain the signals from multiple land covers. The Cropland Data Layer (CDL) dataset is thus utilized to extract target "pure" corn and soybean pixels. The CDL dataset is produced annually by National Agricultural Statistics Service (NASS), United States Department of Agriculture (USDA), and contains spatial distribution information of a number of major crop types at 30 m spatial resolution (Boryan et al., 2011). The yearly CDLs are downloaded and resampled to the spatial resolution of the MODIS MCD43A4 product. The resampled pixels with the fractions of corn or soybean over 90% are selected as target pixels to generate pre-processed smoothed NDVI time series (i.e., target NDVI time series).

Throughout the US, the most comprehensive and publicly accessible crop ground phenological reference data are the crop progress reports (CPRs), published by USDA (NASS CPR, 2020). The CPRs in Illinois provide the cumulative percentages of major crop types (e.g., corn or soybean) that reach certain phenological stages at both ASD- and state-levels, and are updated weekly throughout the growing season. The corn phenological stages recorded in the CPRs include planted, emerged, silking, dough, dented, mature, and harvested stages. As for soybean, the phenological stages in the CPRs are planted, emerged, blooming, setting pods, turning yellow, dropping leaves, and harvested stages. These stages are systematically and consistently monitored by the trained field

observers of USDA based upon the USDA phenological terms and definitions (Table S1). All these critical phenological stages are taken into account for phenological retrieval in this study. The CPRs at the ASD level of Illinois from 2002 to 2017 are employed as the phenological reference data to validate the satellite-derived crop phenological transition dates.

3. Methods

In this study, we propose to devise a hybrid phenology matching model to retrieve a diverse range of crop phenological stages (Section 3.1). The hybrid modeling scheme follows the phenology matching concept through aligning the phenological pattern of target NDVI time series with that of a priori reference shape. With the aligned patterns, it then transforms the pre-calibrated reference phenological transition dates on the reference shape to those on the target NDVI curve for phenological characterization. As the benchmark phenology matching method, the SMF method is briefly introduced in Section 3.2. To better understand the effects of the reference shapes and dates on phenology matching, we design four CPR-based phenological reference scenarios (i.e., year- and region-adjusted, year-adjusted, region-adjusted, and base scenarios) that represent different levels of calibrated reference phenological information (Section 3.3). The performance of the hybrid model is then evaluated and compared to that of the SMF method under various reference scenarios. Fig. 2 shows the flowchart of this study.

3.1. Hybrid phenology matching model

The hybrid phenology matching model integrates the designs of phenometric extraction methods and phenology matching models. Phenometric extraction methods mostly take advantage of the changing characteristics of the NDVI time series to detect the curve landmarks with distinct curve properties (e.g., inflection points) for phenological characterization. Phenology matching models leverage a priori phenological reference to retrieve target critical phenological stages, through matching the phenological patterns of the reference and target curves. The hybrid model synthesizes characteristic landmarks with predefined/calibrated shape and date references to characterize phenological patterns of crop NDVI time series on a per-pixel basis, and to estimate corresponding phenological transition dates (Fig. 3). The design of varying phenological reference scenarios to define the reference shapes and calibrate the reference dates is introduced in Section 3.3. The hybrid model comprises two key components, namely landmark registration and phenophase matching.

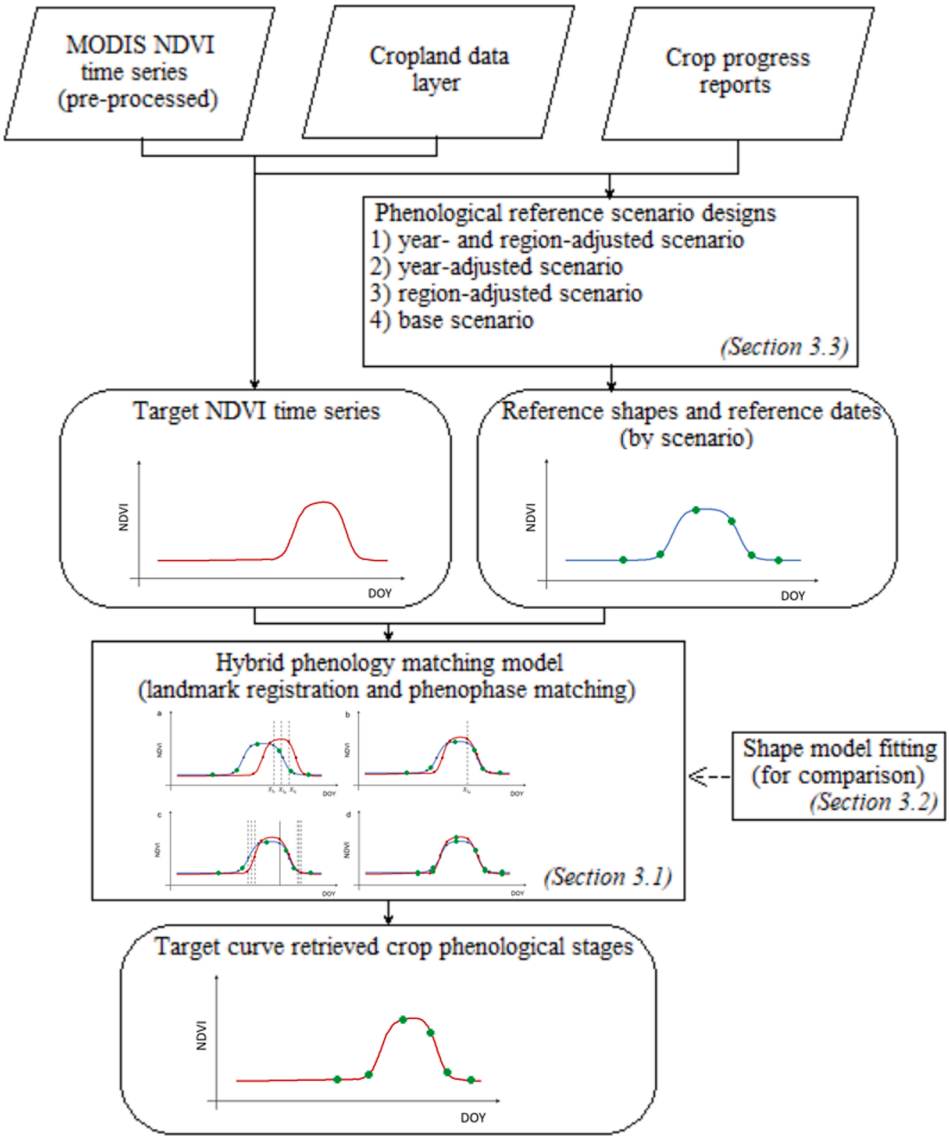

Fig. 2. The flowchart of this study. Four scenarios (year- and region-adjusted, year-adjusted, region-adjusted, and base scenarios) are considered in the assessment.

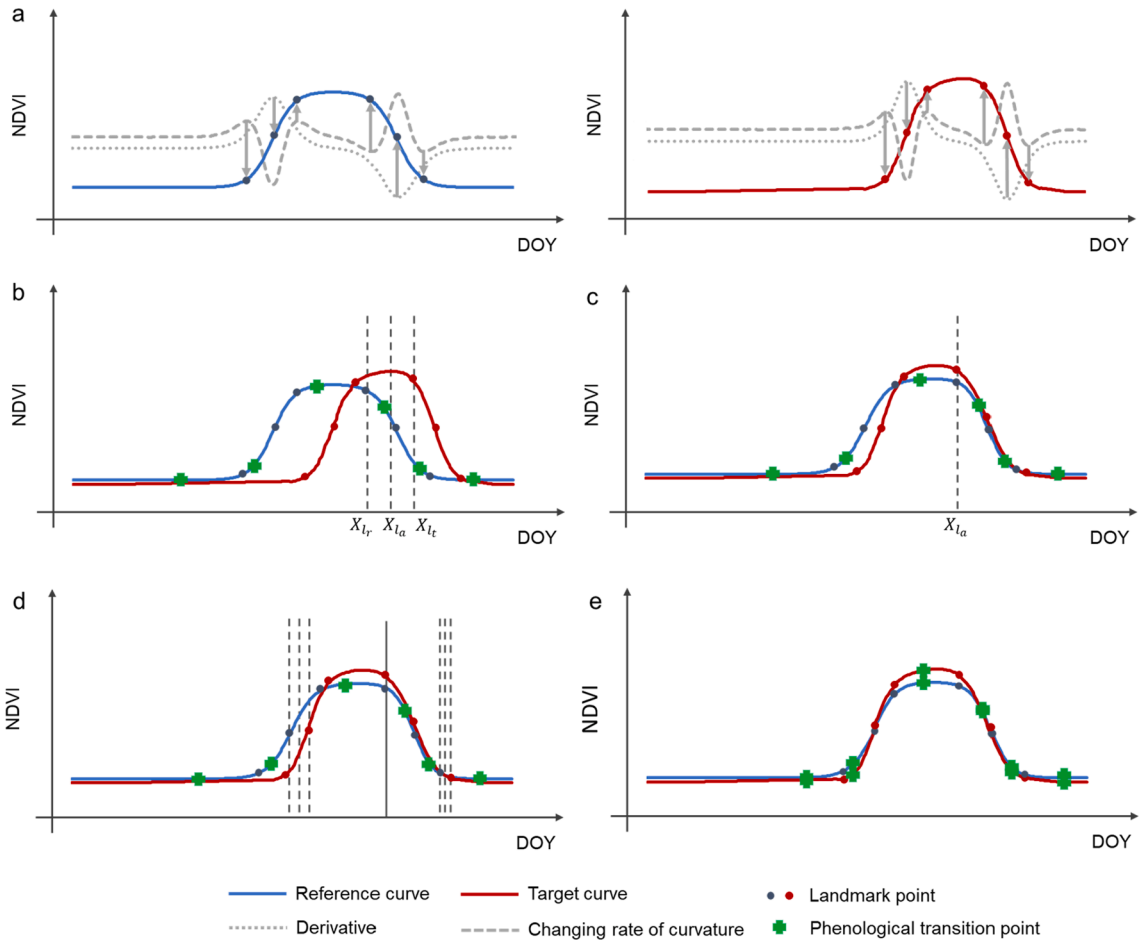

Fig. 3. The hybrid phenology matching model for estimating phenological transition dates of target NDVI time series curves. (a) The landmarks of the target and reference curves are identified using the phenometric extraction methods (e.g., derivative- and curvature-based methods); (b) initial landmark pair is selected on the target and reference curves, respectively; (c) the selected landmark pair is aligned; (d) each curve is partitioned into two intervals by the aligned landmark pair, and the aligning process is repeated within each interval; (e) the two curves are aligned and the phenological transition dates on the target curve can be retrieved. Note the figure is for the illustration purpose. The derivative- and curvature-based curves are not in the same scales as those of target and reference curves, and not all the characteristic landmarks or transition dates are shown in the figure.

The landmark registration component of the model is devised to identify and pair the landmarks of NDVI time series with distinct curve properties. The curve landmarks include local extrema and curve/curvature inflection points, and they characterize the timing of crop undergoing major biophysical and biochemical changes along the phenological development trajectory. The inflection points are identified using two widely utilized phenometric extraction methods, namely the derivative- and curvature-based methods (Diao, 2020). The derivative-based method retrieves the local extremes of the first derivative of the NDVI time series curve as the curve inflection points (Fig. 3a). As the curve derivative measures the extent of changes in crop canopy greenness and photosynthetic activities, the drastic changes captured by the derivative-based inflection points tend to be connected with distinct crop phenological characteristics. Two landmarks can be identified using the derivative-based method. The curvature-based method captures the local extremes in the change rate of the curvature of the NDVI time series as the curvature inflection points (Fig. 3a) (Zhang et al., 2003). Throughout the crop growth cycle, about four curvature inflection points (i.e., greenup, maturity, senescence, and dormancy) that correspond to the rapid changes in the curvature of the time series can be identified. The greenup and maturity points represent the landmarks where the curvature change rate achieves the two local maxima during the upward trajectory of the crop growth cycle. The greenup point denotes the onset of plant photosynthetic activity and the maturity point represents the timing of maximum plant green leaf area. Comparably, the senescence and dormancy points denote the landmarks where the curvature change rate reaches the two local minima of the downward trajectory. The senescence point denotes the onset of decrease of plant photosynthetic activity and the dormancy point represents the timing of plant physiological activity approaching zero. With the phenometric extraction methods, a set of characteristic landmarks are detected for both reference and target time series curves. As crop phenological stages with distinct curve properties maintain relatively stable positions across satellite time series curves (Diao, 2020; Gao et al., 2017), compatible landmarks between the reference and target curves are paired (e.g., greenup of the reference curve paired with greenup of the target curve) for the following phenophase matching.

With the paired landmarks, the phenophase matching component is devised to align the target phenological pattern with that of the reference time series, and to retrieve target phenological transition dates via the matched curves. It employs an innovative phenology matching strategy to selectively align the paired landmarks of the target and reference curves, and to warp corresponding curve intervals for geometrical pattern matching (Fig. 3). This matching strategy follows the multi-interval curve alignment (MICA) algorithm, and progressively aligns the characteristic landmark pairs using a global slope-based distance function (Eq. (1)) (Bender et al., 2012; Mann et al., 2018).

$$d(C_t, C_r) = n^{-1} \sum_{i=1}^{n} |s_i^{C_t} - s_i^{C_r}| \quad (1)$$

Here, C_t and C_r denote a target curve and a reference curve, respectively. C_t is defined by the tuple (X^{C_t}, Y^{C_t}), and X^{C_t} and Y^{C_t} are the x-coordinates and y-coordinates of C_t, respectively. C_r is defined by the tuple (X^{C_r}, Y^{C_r}) accordingly.$s_i^{C_t}$ and $s_i^{C_r}$ represent the slopes of the curves C_t and C_r on the day of year (DOY) i, respectively. n is the number of days in a year. $d(C_t, C_r)$ is the arithmetic mean of the absolute slope differences of the curves C_t and C_r.

The slope-based distance function measures geometrical pattern similarities of the curves, and is invariant to the shift in NDVI values caused by atmospheric interference and instrumental noise. Compared to the NDVI-based distance function, the slope-based distance function emphasizes more on matching the shapes of the target and reference curves, and synchronizing geometrical patterns of crop growth profiles. The landmark pairs are aligned by shifting their respective x-coordinates to the corresponding mean values, and the curves are adjusted accordingly through a warping function $A(X)$ that maps the curve original x-coordinates to the aligned positions. By aligning the landmark pairs and warping corresponding curve intervals, the MICA-based matching strategy seeks to minimize $d\big((A_t(X^{C_t}), Y^{C_t}), (A_r(X^{C_r}), Y^{C_r})\big)$. The warping function $A_t(X^{C_t})$for the target curve C_t is defined as:

$$A_t\left(X_i^{C_t}\right)_{X_{left}\le X_i^{C_t}\le X_{right}} = \begin{cases} X_{l_a} & X_i^{C_t} = X_{l_t} \\ X_{left} + \dfrac{\left(X_i^{C_t} - X_{left}\right)\left(X_{l_a} - X_{left}\right)}{X_{l_t} - X_{left}} & X_i^{C_t} < X_{l_t} \\ X_{right} - \dfrac{\left(X_{right} - X_i^{C_t}\right)\left(X_{right} - X_{l_a}\right)}{X_{right} - X_{l_t}} & X_i^{C_t} > X_{l_t} \end{cases} \quad (2)$$

Here, $X_i^{C_t}$ is the x-coordinate of the curve C_t. X_{left} and X_{right} are the x-coordinates of the start and end points of the curve interval being warped, respectively. l_t and l_r represent a landmark pair to be aligned on C_t and C_r, respectively. When aligning the landmark pair, the x-coordinates of the selected landmarks on C_t and C_r, denoted as X_{l_t} and X_{l_r}, are shifted to their mean x-coordinate X_{l_a} (i.e., $X_{l_a} = (X_{l_t} + X_{l_r})/2$), as shown in Fig. 3c. The x-coordinates of the rest of the curve C_t within the interval are mapped through the warping function, which facilitates the matching of curve phenological patterns as well as the calculation of slope-based curve distance. The warping function $A_r(X^{C_r})$ for the reference curve C_r is defined analogously to $A_t(X^{C_t})$.

As demonstrated in Fig. 3, the MICA-based matching strategy considers the whole curve as one interval (i.e., $X_{left} = 1$ and $X_{right} = n$) during the first round of phenological alignment. Within this initial interval, it searches for an optimal landmark pair, the alignment of which gives rise to the lowest distance $d\big((A_t(X^{C_t}), Y^{C_t}), (A_r(X^{C_r}), Y^{C_r})\big)$ (Fig. 3c). After aligning the first landmark pair, the two curves are each partitioned into two intervals by the aligned landmark pair. The same process is then repeated within each interval until 1) there is no unaligned compatible landmark pair, or 2) aligning the remaining landmark pairs does not lead to a decreased distance (Fig. 3d and 3e).

The phenophase matching of the model iteratively aligns critical landmark pairs that can minimize the slope-based distance between the mapped curve intervals. By leveraging characteristic landmarks, this iterative phenology matching starts with the generic geometrical pattern alignment between the target and reference curves, followed by the fine-tuning of the aligned patterns. It attempts to generate a consensus of aligned phenological patterns, with the matched target and reference curves sharing the same mapped phenological transition dates. Hence the pre-calibrated reference phenological transition dates on the reference curve C_r can be transferred to the aligned target curve C_t (the green dots from Fig. 3b to 3e). The phenological transition dates on the original target curve C_t can then be estimated through the inversion of the warping function $A_t(X^{C_t})$.

As the seasonal growth profiles of the same crop species usually follow comparable phenological patterns, several constraints are employed in the model to restrict curve distortions in phenology matching, as well as to ensure computational efficiency. During the landmark registration, only compatible landmarks (i.e., same type of landmarks from the same phenometric extraction method, such as greenup identified using the curvature-based method) on the target and reference time series profiles can be paired. Considering that varying numbers of landmarks may be detected from the target and reference profiles, the model targets for optimal registration of compatible landmarks, without requiring every landmark pair to be aligned. With a multitude of experiments in reference to previous MICA-based studies, constraints are also applied to interval length, shift in x-coordinates, and warping factor in phenophase matching (Bender et al., 2012; Mann et al., 2018). The minimal interval length is set to be 5% of the length of whole curves of a year, so the model can be more computationally efficient by avoiding aligning intervals that are too trivial. The maximal warping factor is set to be 2, meaning that the length of one interval after alignment cannot be more than two times of its original length. The maximally allowed shift in x-coordinates is set to be 20% of the length of whole curves. The maximal warping factor and maximally allowed shift in x-coordinates together help constrain the distortion of the curves in phenology matching.

The devised hybrid model leverages the complementary strengths of phenometric extraction methods and phenology matching models to achieve more robust and accurate crop phenological retrieval. It integrates characteristic landmarks with phenological references for crop growth stage characterization. The landmark registration preserves the critical curve properties, as well as constrains the curve distortion in geometrical phenological pattern alignment. The phenophase matching further accommodates the relationships between landmarks and reference phenological transition dates. This integrated landmark and reference design not only enables more comprehensive crop phenological pattern matching, but also facilitates the retrieval of the crop phenological stages without distinct curve properties (e.g., planted stage). It may particularly be beneficial for modeling complicated and non-linear phenological patterns with phenological reference and characteristic landmarks. The devised model relaxes the SMF method assumption and can simultaneously retrieve a wide spectrum of crop phenological stages. As the phenological stages are retrieved through the mapping of pre-calibrated reference phenological transition dates, the model also maintains strong potentials to characterize extended physiological growth stages with a priori information of relevant reference transition dates.

3.2. SMF method

For evaluating the hybrid phenology matching model, we compare it to the benchmark SMF method proposed by Sakamoto et al. (2010). This section briefly introduces the SMF method for better understanding. Guided by the geometrical shape concept, the SMF method characterizes target seasonal crop growth patterns through geometrical phenology matching of pre-defined reference shapes (Fig. 4). It assumes that crop phenological patterns embedded in the NDVI time series can be approximated by the geometrical scaling of crop-specific reference shapes, regardless of all the factors that may affect crop growth progress. The SMF method attempts to optimize the scaling parameters that geometrically fit the reference shape to the target NDVI time series. The phenological transition dates of the time series can then be estimated using the optimum scaling parameters and pre-calibrated reference dates. The SMF method focuses on characterizing macroscopic scaling features that can conduct the phenological shape and pattern matching, as well as diminish the influence of localized fluctuations. The geometrical scaling process of the SMF method is defined as:

$$C_f(x) = yscale \cdot C_r(xscale \cdot (x + tshift)) \quad (3)$$

Here, $C_f(x)$ is the fitted NDVI value from the SMF method on the DOY x, and $C_r(x)$ is the NDVI value of the pre-defined reference curve on the

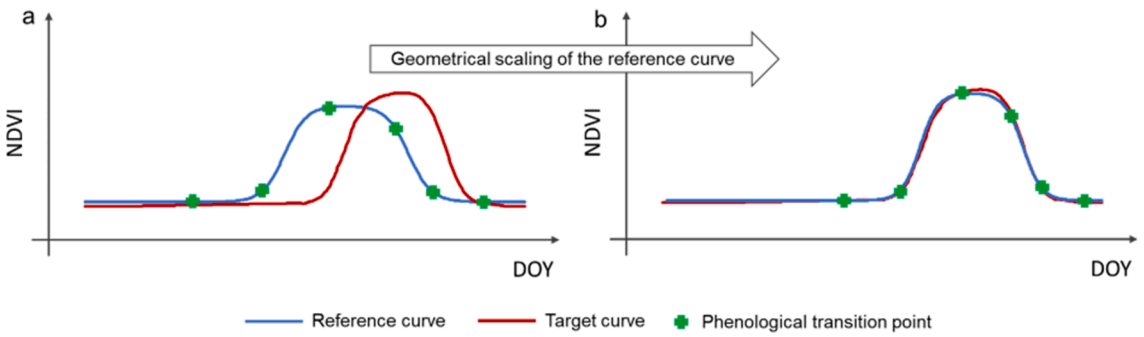

Fig. 4. The SMF method for estimating phenological transition dates of target NDVI time series curves.

DOY *x*. The geometrical scaling process of the reference curve to fit the target time series curve is controlled by the parameters *xscale*, *yscale*, and *tshift*. *xscale* and *yscale* denote the magnitude of stretching or compressing of the reference curve on the horizontal and vertical axes, respectively. *tshift* is the relative shift of crop phenological timing of the reference curve. The combination of the scaling parameters characterizes the phenological difference between the reference and target curves, and enables the geometrical pattern matching to accommodate diverse crop phenological patterns under varying growth conditions over space and time. The scaling parameters are optimized by minimizing the root mean square error (RMSE) between the SMF-fitted curve and the target curve (Eq. (4)).

$$RMSE = \sqrt{\frac{1}{73}\sum_{x=5,10,15,\cdots}^{n}\left(C_f(x) - C_t(x)\right)^2} \quad (4)$$

Here, $C_f(x)$ and $C_t(x)$ denote the fitted NDVI value from the SMF method and the NDVI value of the target curve on the DOY *x*, respectively. *n* is the number of days in a year. With a suite of experiments in reference to previous studies, the searching ranges to optimize the scaling parameters were empirically determined as follows: $0.3 < xscale < 1.5$, $0.3 < yscale < 1.5$, and $-80 < tshift < 80$ (Sakamoto et al., 2010).

With the optimum scaling parameters and pre-calibrated reference dates, the phenological transition dates on the target curve are estimated through the geometric conversion equation (Eq. (5)).

$$X^{C_r} = xscale_{opt}(X^{C_f} + tshift_{opt}) \quad (5)$$

Here, X^{C_f} and X^{C_r} are the estimated phenological transition dates on the target curve, and the pre-calibrated reference dates on the reference curve, respectively. $xscale_{opt}$ and $tshift_{opt}$ are the optimum scaling parameters derived from the SMF method. Comparable to the hybrid model, the SMF method transfers the reference dates from reference curves to target curves for crop phenological retrieval. It can retrieve a range of characteristic phenological stages with the geometrical scaling assumption.

3.3. Design of phenological reference scenarios

With the considerable role of reference shapes and reference dates in phenology matching, the design and characteristic of phenological reference affect the crop phenological retrieval accuracy. Given the difficulty of collecting year-long field-based crop phenological observations across years and locations, it becomes important and imperative to explore the potential of phenological reference design with publicly accessible phenological information (e.g., CPRs) (Sakamoto, 2018). The ASD-level CPRs on a yearly basis in Illinois provide an ideal source to systematically evaluate the reference designs in phenology matching. With the Illinois CPRs, the crop-specific reference shapes and reference dates can be pre-defined/calibrated for each combination of ASDs and years. The nine ASDs in Illinois, together with 16 mapping years, result in 144 unique year-ASD combinations. Specifically, for each year-ASD combination, the crop-specific reference shape is defined as the individual crop pre-processed NDVI time series curve that is the most comparable to the 90th percentile of all the target NDVI curves of the crop for the given year and ASD. With a range of experiments, the 90th percentile is selected to define the reference shapes that can be representative of crop phenological profiles under optimal growth conditions, as well as robust to potential outlying NDVI curves (Sakamoto et al., 2010). The pinpointing of an individual curve approaching the 90th percentile of all relevant target curves further preserves the crop growth geometrical pattern.

With the defined year-ASD reference shape, the corresponding reference dates are pre-calibrated using the cumulative crop phenological information of the publicly accessible CPRs. For each year-ASD combination, half of the target NDVI curves are randomly selected for reference date calibration, and the other half of the curves are reserved for model testing. During the calibration procedure, the selected target curves are first aligned with the pre-defined reference shape through phenological matching (e.g., hybrid or SMF method), so that the warping relationships between the target curves and the reference shape are established. The phenological transition dates on the target curves can then be estimated through the warping relationship and the reference dates. For each phenological stage, the reference date is calibrated within a searching range of two weeks before and after the median date of that stage in the CPRs. Within the searching range, the calibrated reference date will result in the lowest estimation error of the transition dates on the target curves upon comparison to CPRs. The estimation error is calculated as the RMSE between the CPR-documented cumulative percentages of observation dates and the estimated cumulative percentages of corresponding transition dates. Thus with the yearly ASD-level CPR, the reference dates on the pre-defined reference shape for each year-ASD combination are calibrated by minimizing the difference between the estimated transition date distributions of the calibration data and CPR-documented ones. The calibration of reference dates with publicly accessible CPRs not only overcomes the challenge of collecting representative field-based crop phenological observations, but also facilitates the large-scale crop phenological retrieval over wide geographical regions (Sakamoto, 2018).

The pre-defined/calibrated reference shapes and reference dates for each combination of years and ASDs provide an avenue to systematically evaluate the reference designs in phenology matching, particularly with varying levels of reference phenological information. The level of reference phenological information denotes the extent of the inter-annual and regional crop phenological variations being accommodated in reference designs. In this study, we design four CPR-based phenological reference scenarios with different levels, namely the year- and region-adjusted scenario (scenario 1), the year-adjusted scenario (scenario 2), the region-adjusted scenario (scenario 3), and the base scenario (scenario 4) (Table 1 and Fig. 5). Scenario 1 accommodates both the inter-annual and regional crop phenological variations in the reference designs. Under scenario 1, the crop growth reference patterns are assumed to be unique across both years and ASDs. The

Table 1
Design of four phenological reference scenarios using NASS CPRs.

Scenario	Reference Shape	Reference Date	NASS CPR	Calibration Level	Reference Design Assumption
Scenario 1	Year- and ASD-adjusted	Year- and ASD-calibrated	CPR data for all years and ASDs	Accommodate both inter-annual and regional crop phenological variations in reference designs	The crop growth reference patterns are unique across years and ASDs
Scenario 2.1	Year-adjusted, central ASD	For each year, central ASD calibrated	CPR data for all years of central ASD	Accommodate inter-annual crop phenological variations in reference designs	The crop growth reference patterns are unique across years, but can be shared across ASDs for each year
Scenario 2.2	Year- and ASD-adjusted	For each year, central ASD calibrated, other ASDs transferred			
Scenario 3.1	Year 2006, ASD-adjusted	For each ASD, year 2006 calibrated	CPR data for all ASDs in 2006	Accommodate regional crop phenological variations in reference designs	The crop growth reference patterns are unique across ASDs, but can be shared across years for each ASD
Scenario 3.2	Year- and ASD-adjusted	For each ASD, year 2006 calibrated, other years transferred			
Scenario 4.1	Year 2006, Central ASD	Central ASD in 2006 calibrated	CPR data for central ASD in 2006	Not accommodate either inter-annual or regional crop phenological variations in reference designs	The crop growth reference patterns are shared across years and ASDs.
Scenario 4.2	Year- and ASD-adjusted	Central ASD in 2006 calibrated, other year-ASD combinations transferred			

Fig. 5. Design of four phenological reference scenarios with varying levels of phenological calibrations. The reference shapes in green denote that the corresponding reference dates are calibrated for the associated year-ASD combinations. The reference shapes in yellow denote that the corresponding reference dates are not calibrated, but transferred for the associated year-ASD combinations. (For interpretation of the references to colour in this figure legend, the reader is referred to the web version of this article.)

phenological reference information is available for all the years and all the ASDs, and each year-ASD combination has its own reference shape and reference dates. The target curves in the specific year and ASD are matched to the corresponding year-ASD phenological reference for transition date estimation. This scenario can be applied to downscale crop growth stages from the ASD level to a finer scale, such as large fields or county-level statistics.

Scenario 2 only accommodates the inter-annual phenological variations in the reference designs. The crop growth reference patterns under this scenario are assumed to be unique across years, but can be shared across ASDs for each year. We design this scenario by assuming that only one ASD's CPRs for all the years are available, and select the central ASD for phenological reference with consideration of its geographical location, environmental conditions, and farming practices. Only the reference dates in the central ASD for all the years can be calibrated in this scenario. As the reference shapes are defined using satellite time series profiles, the reference shapes of ASDs are not subject to the availability of corresponding CPRs. To further test the role of reference shapes in reference designs, we devise two sub-scenarios (scenario 2.1 and scenario 2.2) in scenario 2. Scenario 2.1 is the year-adjusted, central ASD scenario, of which the reference shape and reference dates calibrated for the central ASD of a year serve as the phenological reference for all the ASDs of the same year. The reference shapes of the other ASDs are not considered in this sub-scenario. Scenario 2.2 is the year-adjusted, ASD transferred scenario, of which the reference dates calibrated for the central ASD of a year are transferred to other ASDs of the same year, based on corresponding reference shapes and phenology matching strategies (hybrid or SMF method). Besides the central ASD, other ASDs have their own year-specific reference shapes and transferred reference dates. Scenario 2 can be applied when the CPRs from the same year are available from the neighboring district.

Scenario 3 only accommodates the regional phenological variations in the reference designs. Under this scenario the crop growth reference patterns are assumed to be unique across ASDs, but can be shared across years for each ASD. We design this scenario by assuming that the ASD-level CPRs are only available in one year, and select the year 2006 for phenological reference as the reference shapes of 2006 are mostly in the middle of reference shapes of all the years. Only the reference dates for the ASDs of the year 2006 can be calibrated in this scenario. Similar to scenario 2, we further devise two sub-scenarios (scenario 3.1 and scenario 3.2) to test the role of reference shapes. Scenario 3.1 is the region-adjusted, year 2006 scenario, of which the reference shape and reference dates calibrated for an ASD of 2006 serve as the phenological reference for this ASD of all the years. The reference shapes of the other years are not considered in this sub-scenario. Scenario 3.2 is the region-adjusted, year transferred scenario, of which the reference dates calibrated for 2006 of an ASD are transferred to other years of the same ASD, based on corresponding reference shapes and phenology matching strategies. Besides the year 2006, the other years have their own ASD-specific reference shapes and transferred reference dates. Scenario 3 could be applicable for a region to use CPRs from historical years for the current year, similar to crop phenology mapping within the season.

Scenario 4 does not accommodate either inter-annual or regional phenological variations in the reference designs. The crop growth reference patterns are shared across both years and ASDs. We design this base scenario by assuming that the CPR is only available for one ASD of one year, and select the central ASD of year 2006 for phenological reference. Only the reference dates for the central ASD of the year 2006 can be calibrated in this scenario. This scenario has a minimum requirement of the reference shape and dates, and is comparable to previous phenology matching studies that used limited field observations as phenological reference to extract crop phenology over large areas (Sakamoto et al., 2010). Similar to scenarios 2 and 3, we further design two sub-scenarios (scenario 4.1 and scenario 4.2) to assess the role of reference shapes. Scenario 4.1 is the base, 2006-central ASD scenario, of which the reference shape and reference dates calibrated for the central ASD of 2006 serve as the phenological reference for all the ASDs and years. The reference shapes except the central ASD of 2006 are not considered in this sub-scenario. Scenario 4.2 is the base, year-ASD transferred scenario, of which the reference dates calibrated for the central ASD of 2006 are transferred to all other year-ASD combinations, based on corresponding reference shapes and phenology matching strategies. Besides the central ASD of 2006, all other year-ASD combinations have their own reference shapes and transferred reference dates. It is noted that the purpose of the study is not to exhaust all the reference scenario designs, but to investigate the performance of phenology matching with representative phenological references. Specifically, the performance of the hybrid model under scenario 1 will be presented in section 4.1, and its performance under other scenarios will be in section 4.2. The comparison results of the performance of the hybrid and SMF methods under all the scenarios will be in section 4.3. At large scales, the levels of publicly accessible phenological information may vary across years and locations. Those reference scenario designs will shed light on the influence of characteristics of reference shapes and dates on phenology matching.

3.4. Accuracy assessment

As the CPRs are collected at the ASD level, our model predictions for the corn (or soybean) target curves that are not employed for phenological calibrations are aggregated accordingly to the ASD level for accuracy assessment. For each year-ASD combination, the predicted median dates of the seven phenological stages of corn (or soybean) are compared with the reference median dates of the corresponding stages from the CPRs. For each phenological stage, a total of 144 data points (9 ASDs by 16 years) are utilized to calculate the R-squared and RMSE values. The R-squared measures the proportion of the variance in the reference median dates of the CPRs explained by the corresponding predicted median transition dates, and the RMSE measures the errors (in days) of the predictions. The spatio-temporal patterns of those accuracy measures across ASDs and years are also explored. To evaluate the influence of various scenario settings of reference shapes and dates on the phenological retrieval accuracy, we further examine the differences in the calibrated reference dates under the four devised scenarios, and compare the RMSE and R-squared values among those scenarios.

4. Results

4.1. Hybrid model-retrieved phenological characteristics

The phenological transition dates of the testing target time series curves for both corn and soybean are retrieved using the hybrid model, and summarized to the ASD level to be compared to corresponding reference CPRs. As the year- and region-adjusted scenario (scenario 1) represents the ideal phenological reference scenario and yields the highest retrieval accuracy, only the phenological results under scenario 1 are presented in section 4.1 to demonstrate the performance of the hybrid model. The performance of the hybrid model under other scenarios will be presented in section 4.2. For each year-ASD combination, the predicted median transition dates of crop phenological stages are compared against the reference median dates of crops going into those stages in the CPRs (Fig. 6). For both corn and soybean, the retrieved and reference median pairs are close to the 1:1 line (the solid diagonal line), which indicates the good performance of the hybrid model in estimating most of phenological stages across ASDs and years, particularly for the emerged, silking, and dough stages of corn, and emerged, blooming, turning yellow, and dropping leaves stages of soybean. The median planting dates for both corn and soybean are accurately predicted for most of ASDs and years. The differences between the retrieved and reference median dates for most of the stages are within 5 days. Compared to other stages, the harvested stages tend to have larger date differences, partly attributable to more variations in crop harvest

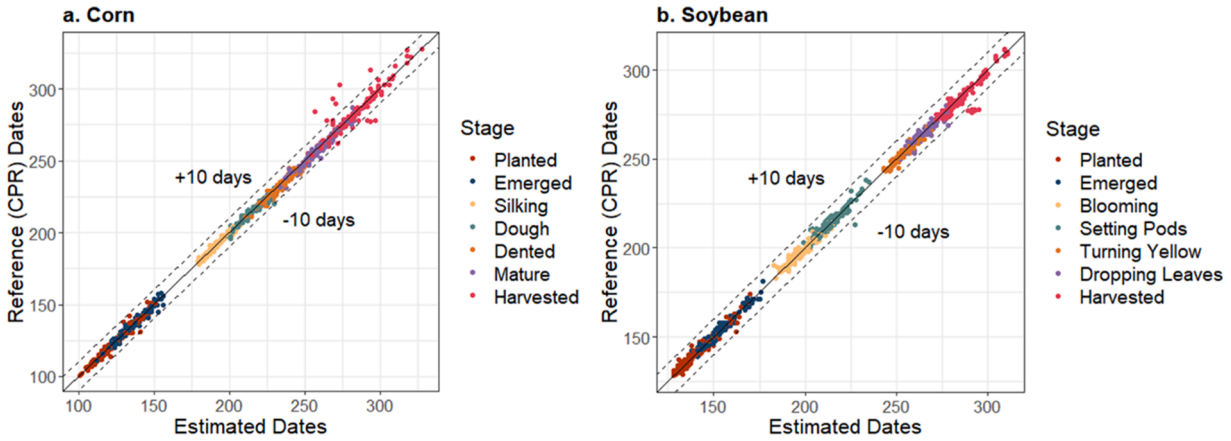

Fig. 6. Scatterplots of the hybrid model-retrieved versus CPR-based reference median transition dates for each year-ASD combination.

management practices among farms.

With the retrieved and reference median pairs, the RMSE and R-squared values of all the phenological stages of corn and soybean are further calculated (Fig. 7). Overall, the hybrid model generates satisfactory results, with RMSEs of the first six stages of both corn and soybean around 2 days and R-squared of those stages higher than 0.9. As regards corn, the retrieved transition dates of the silking stage yield the lowest errors (RMSE = 1.35 and R-squared = 0.97), while the retrieved harvested transition dates give the highest errors (RMSE = 5.99 and R-squared = 0.85). The RMSEs of other estimated transition dates are from 1.9 to 2.5 days, and the corresponding R-squared values range from 0.95 to 0.97. For soybean, the retrieved harvested transition dates generate the highest errors (RMSE = 3.96 and R-squared = 0.83), while the transition dates of all other stages achieve R-squared values ranging from 0.91 to 0.96, and RMSEs from 1.67 to 2.31 days. With the devised hybrid model, more than 80 percent of variability in the ground-based median transition dates in the CPRs can be explained by the model retrieved median dates under appropriate calibration of reference shapes and dates (R-squared from 0.85 to 0.97 for corn, and from 0.83 to 0.96 for soybean). For most of the stages, the average of the difference between the model retrieved and ground-based phenological measures is less than 2.5 days. In particular, the hybrid model demonstrates strong

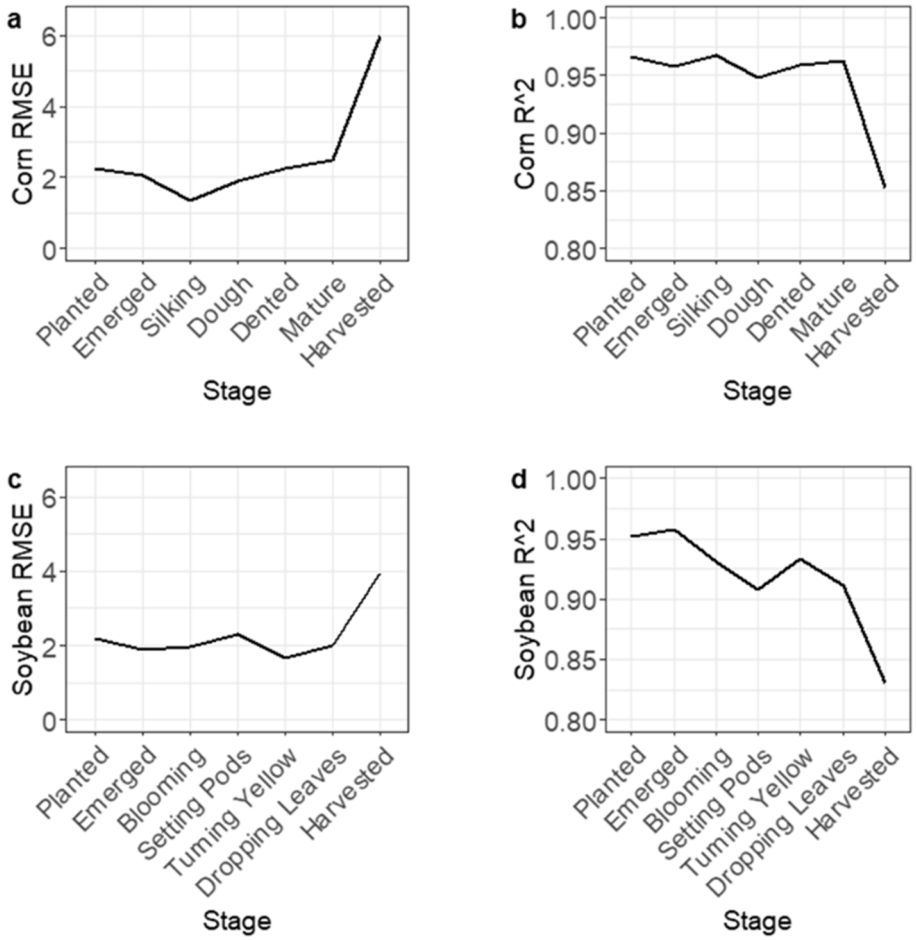

Fig. 7. The RMSE and R-squared values of the hybrid model for corn and soybean under scenario 1 by crop phenological stage.

potentials to directly estimate crop planting dates. The RMSE values for the corn and soybean planted stages are 2.26 days and 2.19 days, respectively. On the other hand, the harvested stage retrieval shows relatively large errors for both crops, as reflected in both Fig. 6 and Fig. 7. Though these two farming practice-relevant stages are both influenced by a variety of factors, the planting of crops is primarily determined by soil and weather conditions. Yet the harvesting of crops is subject to human decisions (e.g., harvest capability and logistics) with more farm-level uncertainties and variabilities.

From 2002 to 2017, the inter-annual phenological patterns captured by the hybrid model correspond well with those in the CPRs (Fig. 8). A variety of cropping conditions and associated crop phenological development trajectories during the study period are characterized by the devised model. The relatively late dates for corn and soybean entering respective phenological stages in 2008 and 2009 are reflected in both hybrid model-estimated results and CPRs. Due to heavy rainfall, wet soil, and cool temperatures, both corn and soybean were planted late during the spring of years 2008 and 2009. The delayed planting affected the timings of the crops going into subsequent growth stages. In 2012, the warm and dry weather prompted earlier planting of corn and the earlier transition dates of its corresponding growth cycle, as revealed in both hybrid model-derived estimates and CPRs. The hybrid model can accommodate the inter-annual variations in crop phenology, as well as characterize varying inter-annual patterns for different phenological growth stages. For instance, the planted stages of corn and soybean exhibit U-shape patterns from 2002 to 2009, due to changing environmental conditions and farming practices. These inter-annual patterns of early phenological stages are yet diluted in succeeding phenological stages. The diverse and complicated yearly patterns across crop phenological stages emphasize the importance of directly retrieving phenological transition characteristics of each individual stage. By accommodating the inter-annual and regional crop phenological variations in the phenological reference design, the hybrid model under scenario 1 achieves high estimation accuracies for a range of corn and soybean phenological stages, and reconciles with CPRs in revealing the characteristic phenological patterns across years in Illinois.

4.2. Four phenological reference scenarios

Four CPR-based phenological reference scenarios with varying levels of phenological calibrations are devised to systematically evaluate the reference designs in phenology matching. With the hybrid model, the crop phenological retrieval accuracies differ among the scenarios (Fig. 9). The year- and region-adjusted scenario (scenario 1) achieves the highest estimation accuracy of all the phenological stages of corn and soybean, emphasizing the importance of accommodating the inter-annual and regional phenological variations in reference designs. Under scenario 1, the RMSEs of most of the corn and soybean stages are around 2 days. With the unique reference shapes and calibrated reference dates for each year and ASD combination, the reference design under scenario 1 takes into account the spatio-temporal differences in crop growing and management conditions, including climate, soil properties, crop varieties, and cultivation methods.

Under scenarios 2, 3, and 4, two corresponding sub-scenarios are devised to assess the role of reference shapes in reference designs. The comparisons between scenarios 2.1 and 2.2, between scenarios 3.1 and 3.2, and between scenarios 4.1 and 4.2, demonstrate that transferring the reference dates of limited calibration to formulate year-ASD specific phenological reference does not improve the model performance. The RMSEs are larger after transferring the reference information in each sub-scenario for almost all the phenological stages of both corn and soybean. Though the reference shapes can be uniquely pre-defined for each year-ASD combination with satellite time series, the lack of calibrated reference dates for certain years or ASDs may not be compensated by corresponding transferred reference dates using reference shapes and the hybrid model. On one hand, the transferred phenological references tend to share comparable phenological characteristics with corresponding calibrated phenological references designed in each scenario, as the transferred reference dates stem from the calibrated reference dates with phenology matching. The transferred phenological references may not represent the characteristic crop phenological development for the target year-ASD combinations, which may possess different crop growing and management conditions. On the other hand, the transferring process may bring additional uncertainties and errors into

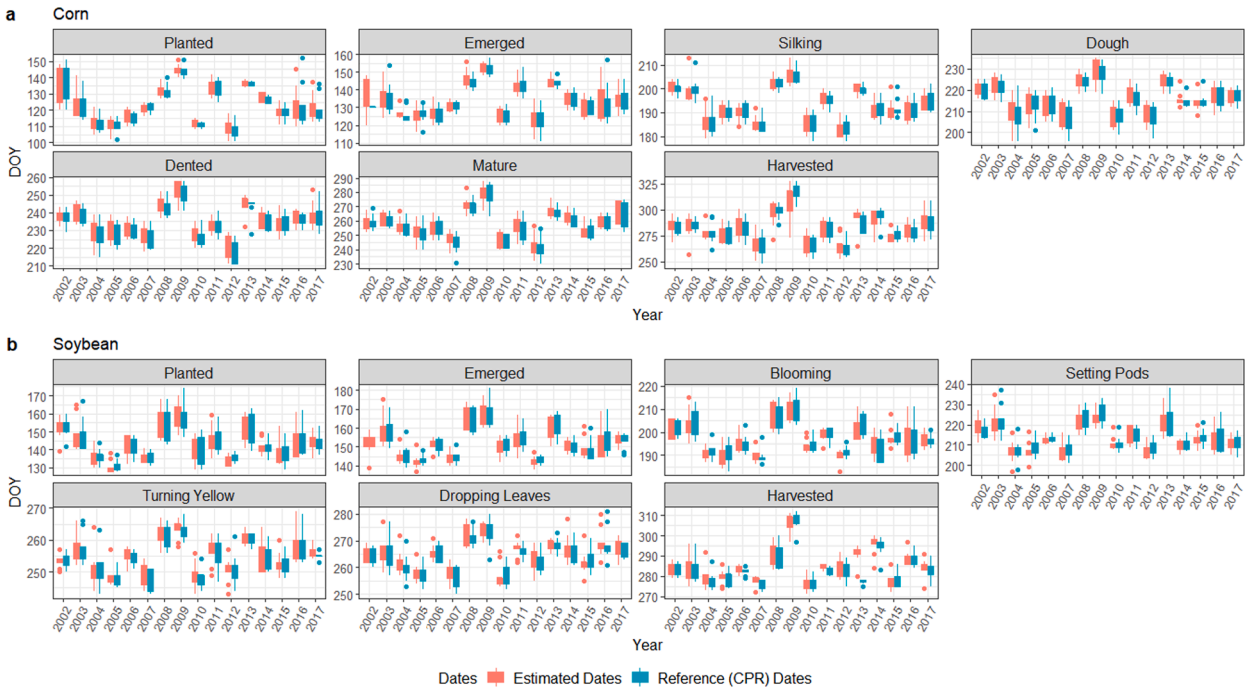

Fig. 8. Inter-annual comparisons between the hybrid model-estimated transition dates and CPR-based reference transition dates of phenological stages of corn and soybean in Illinois.

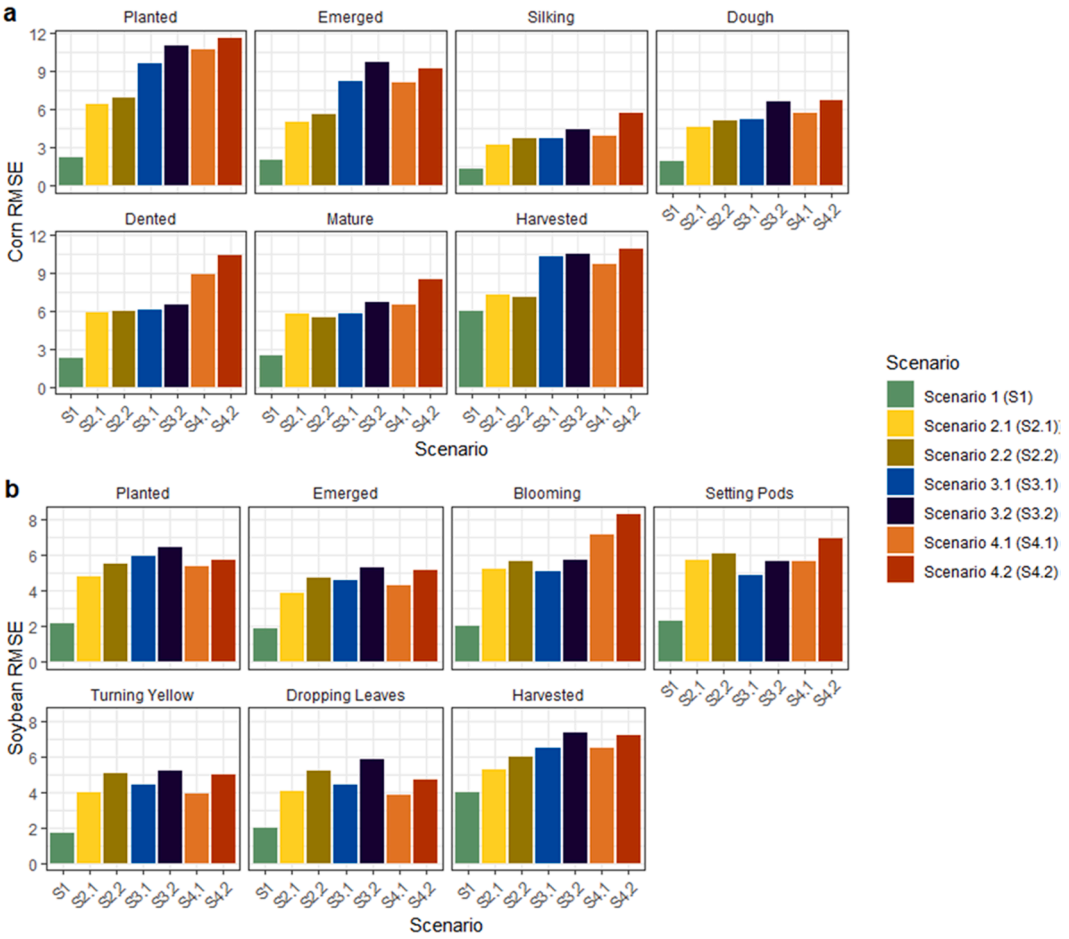

Fig. 9. Comparisons of RMSEs of the hybrid model under four phenological reference scenarios for (a) corn and (b) soybean.

subsequent transition date estimations, attributing to the underperformance of each transferred sub-scenario. Since the performance of the hybrid model does not benefit from the transferred phenological references, only scenarios 1, 2.1, 3.1, and 4.1 are considered in the following analyses.

Among the scenarios, the year-adjusted scenario (scenario 2.1) performs the next best, with only larger overall transition date estimation errors than scenario 1. The RMSE values under scenario 2.1 range from 3.2 to 7.3 days for the phenological stages of corn, and from 3.9 to 5.7 days for the stages of soybean. The region-adjusted scenario (scenario 3.1) yields generally lower accuracy compared to scenario 2.1, with RMSE values ranging from 3.7 to 10.3 days for corn phenological stages, and from 4.4 to 6.5 days for soybean stages. The base scenario (scenario 4.1) also shows larger RMSEs compared to scenario 2.1, and the RMSEs are from 3.9 to 10.7 days for corn, and from 3.8 to 7.1 days for soybean. With the CPRs, it is ideal to design both year- and region-adjusted phenological reference, with each year-ASD combination maintaining its own reference shapes and calibrated reference dates. Yet compared to region-adjusted phenological reference, the hybrid model with year-adjusted reference tends to attain higher phenological retrieval accuracy in Illinois. The underlying phenological reference designs under those scenarios indicate that the inter-annual changes of crop growing season conditions and phenological development trajectories are more pronounced than the regional phenological variations across ASDs of Illinois. Correcting the year-dependent bias errors under scenario 2.1 is more effective than correcting the region-dependent bias errors under scenario 3.1 for most of the corn and soybean phenological stages in Illinois. The hybrid model under scenarios 3.1 and 4.1 exhibits comparable performance for many phenological stages, indicating that only accommodating the regional phenological variations may not be sufficient to generate more favorable results for our study site. Among the phenological stages, the silking and dough stages of corn, as well as the emerged, turning yellow, and dropping leaves stages of soybean, achieve higher and more consistent retrieval accuracies across the devised scenarios.

We further assess the phenological reference designs by comparing the differences of reference dates of varying levels of calibrations under four devised scenarios. The calibrated reference dates under four scenarios employed for each year-ASD combination are normalized to its pre-defined reference shape using the hybrid model, respectively. As scenario 1 achieves the highest accuracy and the reference dates under this scenario are calibrated individually for each year-ASD combination, the calibrated reference dates of scenario 1 serve as the benchmark for quantifying the reference date differences under varying levels of calibrations. For each scenario, the absolute differences between the scenario-normalized reference dates and corresponding calibrated reference dates of scenario 1 are calculated for each year-ASD combination, and are then averaged across years and ASDs by crop phenological stages (Fig. 10). Upon comparisons with scenario 1, the mean absolute differences (MADs) of calibrated reference dates in scenario 2.1 are less than those in scenarios 3.1 and 4.1 for all phenological stages of corn and soybean. The smaller MADs indicate that the phenological reference design of scenario 2.1 is more similar to that of scenario 1. The variations of phenological stages across years and ASDs are accommodated more by the year-adjusted reference, compared to region-adjusted or base references. The comparable MADs under scenarios 3.1 and 4.1 for most of the corn and soybean stages illustrate the diminishing role of region-adjusted reference in Illinois, resonating with scenario

Fig. 10. Mean absolute differences of the calibrated reference dates across years and ASDs and 95% confidence intervals (yellow error bars) under scenarios 2.1, 3.1, and 4.1, for (a) corn and (b) soybean. For each scenario, the differences are calculated between the scenario-normalized reference dates and corresponding calibrated reference dates of scenario 1. S2.1, S3.1, and S4.1 in the figure denote Scenario 2.1, Scenario 3.1, and Scenario 4.1, respectively. (For interpretation of the references to colour in this figure legend, the reader is referred to the web version of this article.)

performances in Fig. 9.

The average RMSEs of phenological retrieval of each ASD (and each year) are calculated for both corn and soybean under the four scenarios, with corresponding spatial and temporal patterns shown in Fig. 11. For most ASDs and years, the phenological retrieval accuracies decrease from scenario 1 to scenario 3.1 (and scenario 4.1), consistent with Fig. 9 and Fig. 10. In general, the average RMSEs are the smallest under scenario 1 and much larger under scenarios 3.1 and 4.1. The comparable and relatively high estimation accuracies for most ASDs and years under scenarios 1 and 2.1 demonstrate the potential of the hybrid model with appropriate phenological references to characterize spatio-temporal phenological variations of both corn and soybean in Illinois. The divergent patterns in the retrieval accuracies for certain regions and years can be attributed to phenological reference designs and spatio-temporal variations in characteristic phenology. With the central ASD and year 2006 selected for reference designs of limited calibrations, the average RMSEs are generally smaller in this particular region (or year) across scenarios. The delayed crop phenological development in 2009 instead leads to larger estimation errors, especially for scenarios 3.1 and 4.1 where inter-annual phenological variations are not accommodated.

4.3. Comparisons of the hybrid and SMF methods

The hybrid model is further compared with the SMF method for retrieving phenological transition dates under the four scenarios using RMSE and R-squared (Fig. 12). As for corn, the performances of the

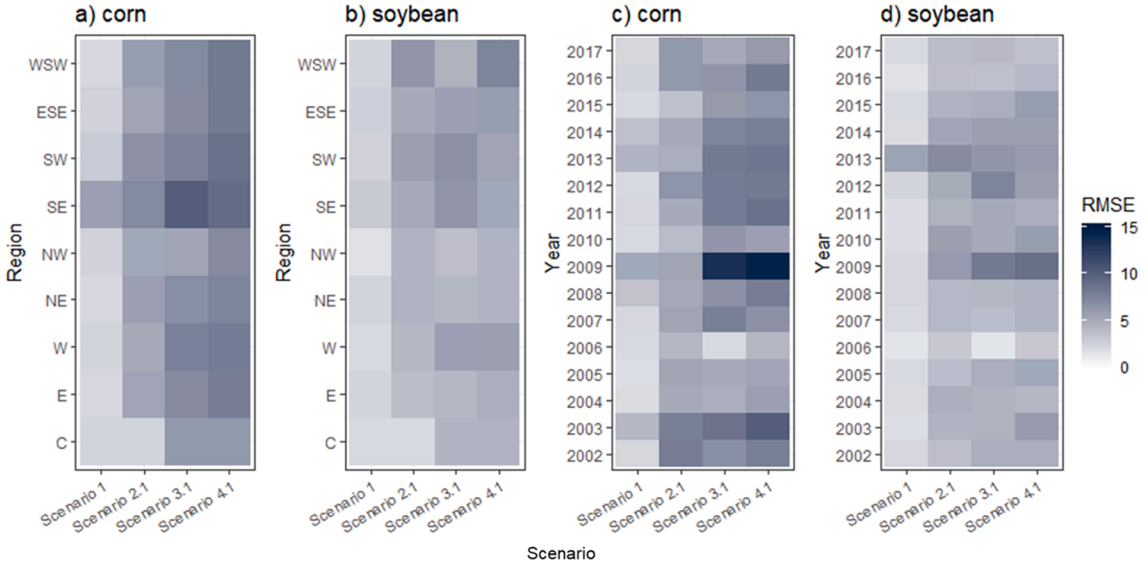

Fig. 11. The average RMSEs of phenological retrieval of each ASD (a and b) and each year (c and d) using the hybrid model for corn and soybean in Illinois.

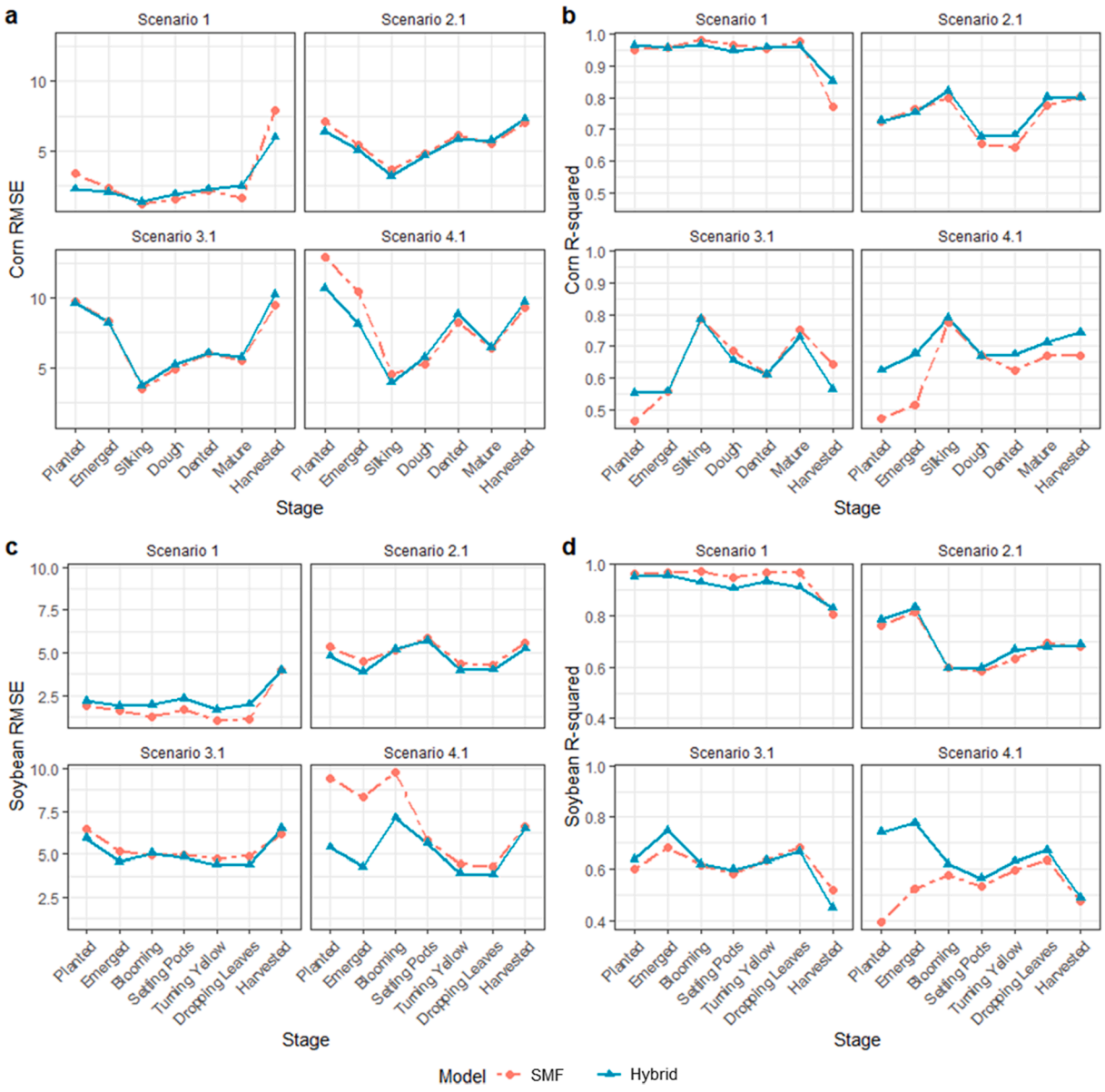

Fig. 12. Comparisons of the hybrid and SMF methods' performances in estimating phenological transition dates for corn and soybean under four phenological reference scenarios.

hybrid and SMF methods are mostly comparable under scenarios 1, 2.1, and 3.1, yet the hybrid model achieves higher R-squared values for the corn harvested stage in scenario 1, the dough and dented stages in scenario 2.1, and the planted stage in scenario 3.1. Under scenario 4.1, the hybrid model attains higher retrieval accuracies for most of the stages in terms of both RMSE and R-squared (Table 2). The RMSEs of the hybrid and SMF methods are 10.71 days and 12.92 days for the corn planted stage, respectively, and are 8.17 days and 10.44 days for the corn emerged stage, respectively. The R-squared values of the hybrid model are higher for almost all the stages of corn, particularly for its planted and emerged stages. With respect to soybean, the hybrid and SMF methods also yield similar performances under scenarios 1, 2.1, and 3.1. Under scenario 4.1, the hybrid model yields consistently higher estimation accuracies for all the stages according to both RMSE and R-

Table 2
RMSE and R-squared values of the hybrid and SMF methods for corn and soybean under scenario 4.1.

Corn Stage	RMSE		R-squared		Soybean Stage	RMSE		R-squared	
	Hybrid	SMF	Hybrid	SMF		Hybrid	SMF	Hybrid	SMF
Planted	**10.707**	12.921	**0.624**	0.472	Planted	**5.402**	9.412	**0.742**	0.393
Emerged	**8.169**	10.442	**0.675**	0.515	Emerged	**4.298**	8.381	**0.777**	0.524
Silking	**3.932**	4.554	**0.790**	0.775	Blooming	**7.149**	9.772	**0.619**	0.576
Dough	5.734	**5.281**	0.669	**0.670**	Setting Pods	**5.645**	5.836	**0.564**	0.531
Dented	8.842	**8.250**	**0.675**	0.624	Turning Yellow	**3.909**	4.464	**0.630**	0.597
Mature	**6.422**	6.469	**0.712**	0.669	Dropping Leaves	**3.830**	4.309	**0.671**	0.633
Harvested	9.721	**9.280**	**0.742**	0.671	Harvested	**6.494**	6.648	**0.488**	0.475

squared, especially for the planted, emerged, and blooming stages. For instance, the RMSEs of the hybrid and SMF methods for the soybean planted stage are 5.40 days and 9.41 days, respectively, and the corresponding R squares of the hybrid and SMF methods are 0.74 and 0.39, respectively. The superior performances of the hybrid model under scenario 4.1 suggest that the devised model is more robust to the decreasing levels of phenological reference calibrations than the SMF method, and is particularly advantageous when the phenological reference information is limited.

Given the interest and importance of directly estimating crop planted stages, we further examine the scatterplots of the hybrid model-retrieved versus CPR-based median planting dates, and the scatterplots of SMF-retrieved versus CPR-based median planting dates, under the four scenarios for corn and soybean (Fig. 13 and Fig. 14). Under scenarios 1 and 2.1, the scatterplots generated by the hybrid and SMF methods are comparable for both corn and soybean. Yet for scenarios 3.1 and 4.1, the hybrid model-based median pairs are less dispersed and closer to the 1:1 diagonal line, associated with higher R-squared values and smaller RMSEs. Compared to SMF, the hybrid model in particular exhibits improved capabilities in predicting soybean planting dates, with most of the median pairs falling within the range of [-10, 10] days differences. The hybrid model also achieves enhanced performance for corn planting date estimation, though the delayed corn planting in certain years and ASDs tends to be estimated earlier, partly due to the deviation of actual corn planting time from the limited phenological references under scenarios 3.1 and 4.1.

Overall, the hybrid and SMF methods share similar patterns in the prediction accuracies across different crop phenological stages. Both methods can better estimate the transition dates of silking and dough for corn, alongside the dates of turning yellow and dropping leaves for soybean. The hybrid and SMF methods attain comparable accuracies when spatio-temporal phenological variations of crops are adequately accommodated in phenological reference designs (e.g., scenarios 1 and 2.1). Yet when the phenological references are of limited calibrations (e.g., scenario 4.1), the hybrid model is more robust and performs particularly better for the crop early phenological stages (e.g., planted and emerged stages). These results demonstrate the potential of the hybrid model in expanding the phenology matching designs for crop stage retrieval, with its ability to accommodate larger discrepancies between the predicted phenological transition dates and the reference ones.

5. Discussion

The hybrid phenology matching model can achieve high accuracies for estimating corn and soybean phenological stages, particularly with the year- and region-adjusted reference shapes and dates. Under scenario 1, the RMSE values for the corn estimated phenological transition dates are less than 6 days, and the R-squared values are higher than 0.85. With regard to soybean, the RMSE values for all the phenological stages are less than 4 days, along with R-squared being higher than 0.83. The inter-annual and regional phenological patterns characterized by the hybrid model correspond well with those in the CPRs. As an innovative phenology matching model, the hybrid model exhibits enhanced capabilities in simultaneously retrieving a wide suite of crop phenological stages, owing to its three unique properties. First, the hybrid model integrates the designs of phenometric extraction methods and phenology matching models. It integrates characteristic landmarks with a priori shape and date references for phenological identification. The integrated landmark and reference design not only enables more effective curve alignment, but also dramatically facilitates the characterization of the crop stages without distinct curve properties (e.g., planted stages). Second, the hybrid model employs the global slope-based distance function to conduct the phenology matching. Compared to the NDVI-based distance function, the slope-based function is particularly advantageous in synchronizing the geometrical patterns of crop growth profiles, as well as accommodating the shifts and fluctuations of NDVI time series across locations and years. Third, the hybrid model is flexible and robust in crop growth pattern matching. Depending on the crop growth profiles, certain types of characteristic landmarks (e.g., local extrema) may or may not be identified. Given varying numbers of landmarks may be identified for the satellite time series profiles, the hybrid model targets for optimal registration of compatible landmarks, without requiring every landmark pair to be aligned. The flexible landmark registration facilitates more comprehensive crop phenological modeling, particularly for non-linear and complicated phenological patterns. It also enhances the hybrid model's robustness to localized

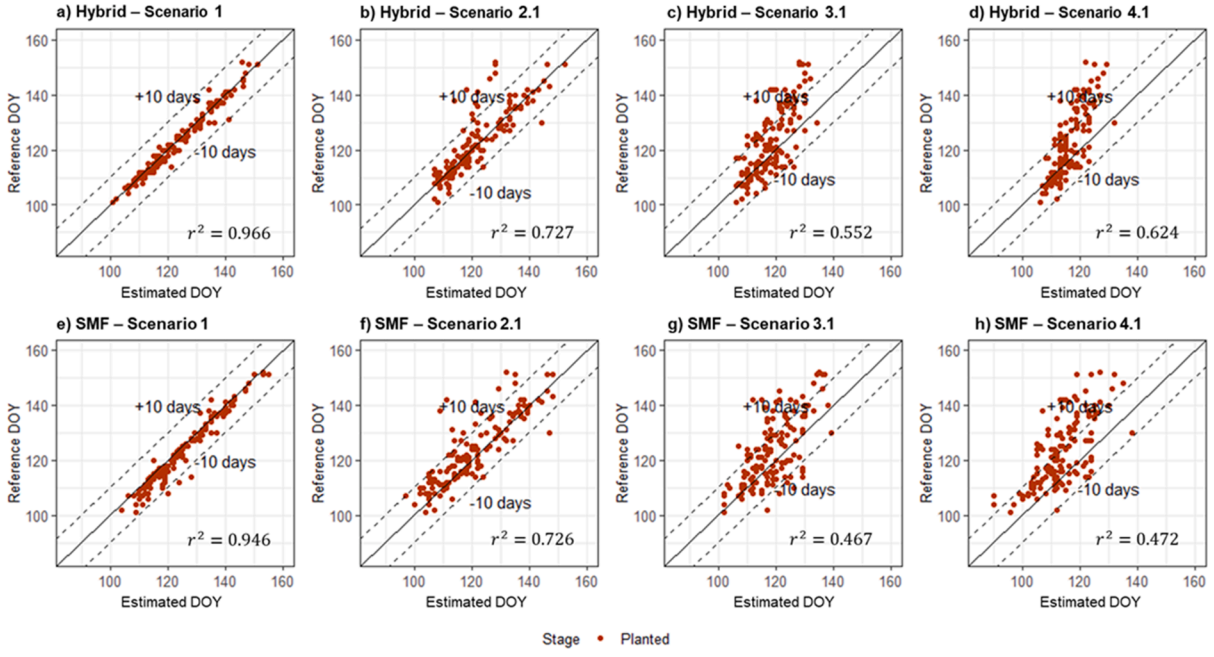

Fig. 13. Scatterplots of the hybrid model-retrieved versus CPR-based median planting dates (a, b, c, and d), and SMF-retrieved versus CPR-based median planting dates (e, f, g, and h) for corn under four scenarios.

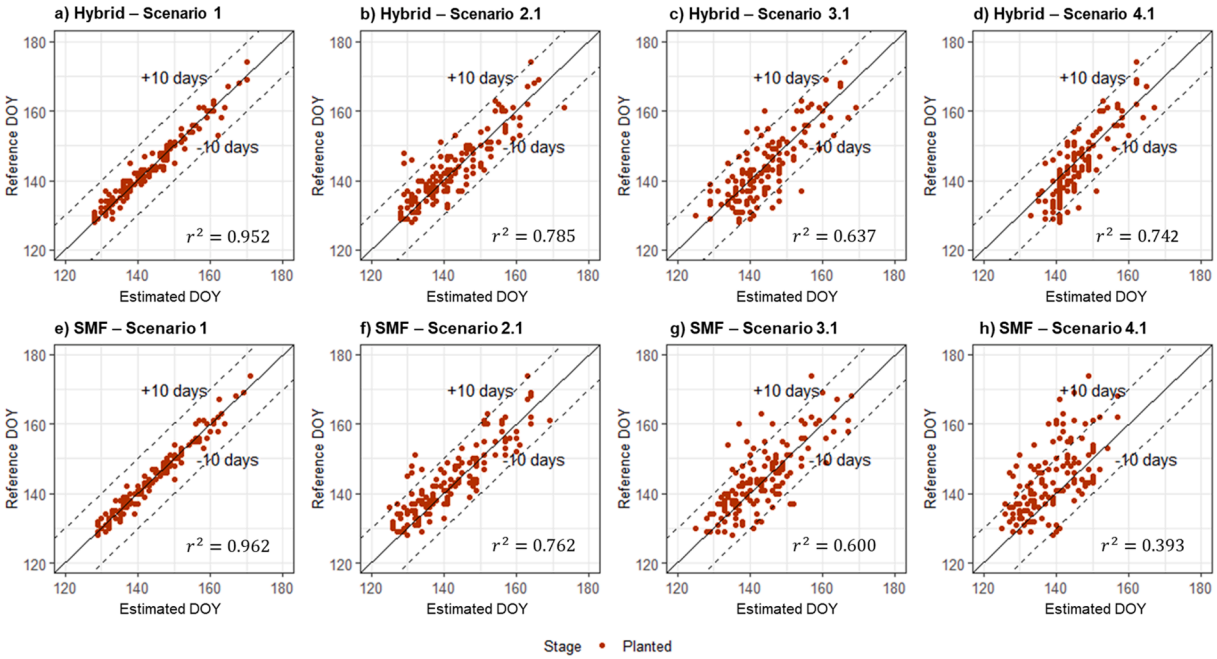

Fig. 14. Scatterplots of the hybrid model-retrieved versus CPR-based median planting dates (a, b, c, and d), and SMF-retrieved versus CPR-based median planting dates (e, f, g, and h) for soybean under four scenarios.

non-vegetation-related fluctuations and noises in the satellite time series, with the model achieving comparable performances for smoothed and unsmoothed NDVI time series under devised scenarios (see Fig. S1 and Fig. S2 for details). As the landmarks affected by the noises may not help with crop geometrical pattern matching, they may not be targeted for optimal registration and may be left unaligned.

The devised four phenological reference scenarios illustrate that the calibration procedures of reference phenological transition dates on reference shapes exert a significant role in determining the retrieval accuracies of the hybrid model. Among the scenarios, the hybrid model under the year- and region-adjusted scenario is the most superior across all the phenological stages in terms of RMSE and R-squared for both corn and soybean. It can capture most of the variability in the median phenological transition dates of the CPRs, with its predicted dates comparable to the observed ones. Calibrating the hybrid model with such rich CPR-enabled phenological information is favored for accurate characterization of crop growing progress. The year-adjusted scenario can lead to more accurate phenological retrieval than the region-adjusted and base ones. The crop growth profiles and associated characteristics (e.g., planted and harvested stages) exhibit more inter-annual phenological variations than the regional variations of a year, as climate conditions and farming practices tend to differ more from year to year in Illinois. The performance of the region-adjusted scenario is mostly similar to that of the base scenario. It is yet noted that the phenological scenario designs tested for Illinois in this study may diminish the role of region-adjusted phenological references in the hybrid model, as crop phenological characteristics within the extent of Illinois may not vary dramatically for a single mapping year. Further inspections of reference designs over extended geographical regions would be desired in future studies for more comprehensive evaluations. With the combined satellite time series and CDLs, the reference shapes can potentially be defined for each ASD and year. The reference dates with varying calibration levels can be defined according to CPRs. Yet the increased RMSEs induced by transferred reference dates under scenarios 2–4 emphasize the importance of appropriately calibrated reference dates on reference shapes, particularly the ones that can accommodate the inter-annual phenological variations. Overall, the phenological calibration process through publicly accessible CPRs enables the hybrid model to reveal the characteristic spatio-temporal patterns of a variety of crop growth stages, without requiring long-term field phenological observations. The phenological reference scenario designs are also instructional in formulating appropriate reference shapes and dates for phenological retrieval over other geographical regions, which may be subject to varying levels of publicly available phenological information.

Among the phenological stages, the silking and dough stages of corn, along with the turning yellow and dropping leaves stages of soybean, can be more accurately estimated (RMSEs around or less than 5 days) by both the hybrid and SMF methods. The performances of these two methods for those stages are relatively robust under different calibration levels of phenological references, partly because the transition dates of those stages maintain relatively stable relationships with characteristic landmarks (e.g., maturity timing) of NDVI time series. Some of those stages do not possess distinct curve properties and might not be accurately predicted by the phenological monitoring framework devised in previous studies (Diao, 2020). For instance, the RMSE of the corn dough stage is around 10 days under the phenological framework, despite with the preferred combinations of curve fitting phenological models (e.g., Beck-based double logistic model) and phenometric extraction methods (e.g., curve derivative).

Beyond the phenological framework, the hybrid and SMF methods can also estimate the transition dates of the planted stage of crops, with RMSEs ranging from around 2 days to 13 days. Compared to the SMF method, the hybrid model is more robust and maintains more advantages in predicting the planted stages, particularly under the base scenario. The SMF method characterizes macroscopic scaling features for reference shape transformation by following the geometrical scaling assumption. It has been found to capture the phenological features near the peak of the crop profiles (e.g., silking stage) better than those near the tails of the profiles (e.g., planted stage) (Sakamoto, 2018). By contrast, the hybrid model focuses on aligning characteristic landmarks that widely spread over the crop profiles and can reduce the effects of the geometrical scaling assumption. The integration of characteristic landmarks and reference phenology not only enables more comprehensive modeling of geometrical patterns of crop growth profiles, but also accommodates the relationships between landmarks and reference transition dates, both of which can facilitate better and more robust

detection of crop planted stages. This integrative modeling design of the hybrid model holds great potential to characterize complicated crop phenological patterns, such as double and multiple growth cycles. By developing the hybrid model, we attempt to expand the phenology matching designs tailored for crop stage characterization, as well as to complement the previously devised phenological monitoring framework. Despite the good performance of the hybrid model, some phenological stages (e.g., dented stage of corn and blooming stage of soybean) can be better estimated by the phenological monitoring framework, particularly under the base scenario. Further synthesizing of the methods in the phenological monitoring framework with the hybrid model would facilitate more comprehensive crop phenological detection.

Defining representative reference shapes and dates is crucial in conducting phenology matching. The devised phenological reference scenarios illustrate the importance of accommodating the inter-annual phenological variations in reference designs. For many crop-producing states, the yearly CPRs are generally available to the public, which can largely facilitate individual calibration of reference shapes and dates from year to year. Yet for other geographical regions with limited cross-year phenological reference, the model performance may be degraded if there is considerable variability in NDVI time series curves across years. As meteorological conditions (e.g., temperature) play an important role in affecting the crop growth and phenological development, combining the crop models with satellite time series profiles may help define environment-based phenological reference. Zeng et al. (2016) improved the SMF method by leveraging the crop models to generate the ground-based phenological reference in terms of accumulated photothermal time (APTT). By taking into account dominant environmental factors (e.g., air temperature and photoperiod), the APTT-based reference information reduces the influence of inter-annual climatic fluctuations to improve the SMF phenological detection accuracy. Yet crop growth is affected by a combination of factors (e.g., water stress, management practices, and crop cultivars), appropriately simulating phenological reference of crop growth profiles in response to a synthesis of environmental factors at large scales is challenging (Zeng et al., 2020). Due to the potential uncertainties from the simulation process, scrutinizing the design of phenological reference in light of various environmental factors is out of the scope of this study, but would be a desired future direction to further improve the hybrid model performance. Additionally, the study is conducted at the MODIS scale to be compatible with that of the phenological framework of our previous study, and to demonstrate the potential of the hybrid model. The hybrid model, along with the methods in the phenological framework, can largely expand our capabilities to estimate a suite of crop growth stages at regional scales, particularly for relatively large farmlands. The recently available harmonized Landsat and Sentinel-2 data, combined with MODIS and Visible Infrared Imaging Radiometer Suite (VIIRS), can further facilitate the crop phenological monitoring at field levels (Bolton et al., 2020; Zhang et al., 2020).

The CPRs released by USDA represent the most comprehensive and systematic ground-based observations of crop phenological progress, and have been widely utilized to validate the remotely sensed phenological measures at the ASD and state levels. We further demonstrate the potential of CPRs in guiding the calibration of reference shapes and transition dates to build representative crop growth profiles under various scenarios. For the regions with only state-level CPRs, the year-adjusted scenario (scenario 2) and the base scenario (scenario 4) devised in the study could be instrumental for relevant phenological reference designs. In recent years, the rapid growth of near surface remote sensing (e.g., unmanned aerial vehicle, PhenoCam, and smart phone-based photos) provides new means to collect crop phenological observations for individual farm fields (Hufkens et al., 2019; Richardson et al., 2018). Those objective field-level phenological observations may further help with the calibration of phenological references and validation of phenological characteristics. Besides, a range of vegetation indices have been developed for agricultural remote sensing, with each emphasizing unique crop properties (Xue and Su, 2017). Further inspection of other vegetation indices, together with near surface remote sensing, will improve the understanding of the devised hybrid model in crop phenological retrievals. The designed hybrid model is a retroactive approach that needs a crop type map (CDL in this study) to define the reference shapes and phenological dates for the target year. Although it could be a challenge to use the retroactive approach within the season due to the limited observations and crop type maps (Gao and Zhang, 2021), the hybrid model in this paper is beneficial for investigating the spatial and temporal variability of crop growth stages and generating statistical reports at finer scales using publically available CPRs.

6. Conclusions

Monitoring the biological lifecycles of crops provides a feasible means to evaluate the agricultural responses to climate change, environmental variability, and farming activities from one phenological stage to another. In this study, we develop an innovative hybrid phenology matching model that can robustly detect a range of crop growth stages under different phenological reference scenarios. With its integrative landmark and reference design, the hybrid model demonstrates enhanced capabilities in characterizing the phenological stages without distinct curve properties. In Illinois, the hybrid model with the year- and region-adjusted phenological reference can identify the median transition dates of most phenological stages of corn and soybean with R-squared higher than 0.9 and RMSEs less than 5 days. Compared to the SMF method, the hybrid model exhibits better and more robust performance particularly in retrieving the crop planting dates, and promises to capture complicated phenological patterns with the relaxed geometrical scaling assumption. The characteristic spatio-temporal patterns of crop planting dates can help construct more accurate crop simulation models and design proactive adaptation strategies of crop planting under varying environmental conditions. The hybrid model expands the phenological monitoring framework, as well as phenology matching designs. This innovative hybrid phenology matching model, together with CPR-enabled phenological reference calibrations, holds large potential in revealing spatio-temporal patterns of crop phenology over extended geographical regions.

Declaration of Competing Interest

The authors declare that they have no known competing financial interests or personal relationships that could have appeared to influence the work reported in this paper.

Acknowledgements

Funding support for this research is provided by the National Science Foundation (grant number 1849821), the United States Department of Agriculture (grant number 2021-67021-33446), and the National Aeronautics and Space Administration (grant number 80NSSC21K0946). This research is part of the Blue Waters sustained-petascale computing project, which is supported by the National Science Foundation (awards OCI-0725070 and ACI-1238993) the State of Illinois, and as of December, 2019, the National Geospatial-Intelligence Agency. Blue Waters is a joint effort of the University of Illinois at Urbana-Champaign and its National Center for Supercomputing Applications.

Appendix A. Supplementary material

Supplementary data to this article can be found online at https://doi.org/10.1016/j.isprsjprs.2021.09.011.

References

Abendroth, L.J., Elmore, R.W., Boyer, M.J., Marlay, S.K., 2011. Corn growth and development. PMR.

Bender, B.J., Mann, M., Backofen, R., Spiecker, H., 2012. Microstructure alignment of wood density profiles: an approach to equalize radial differences in growth rate. Trees 26 (4), 1267–1274.

Bolton, D.K., Friedl, M.A., 2013. Forecasting crop yield using remotely sensed vegetation indices and crop phenology metrics. Agric. For. Meteorol. 173, 74–84.

Bolton, D.K., Gray, J.M., Melaas, E.K., Moon, M., Eklundh, L., Friedl, M.A., 2020. Continental-scale land surface phenology from harmonized Landsat 8 and Sentinel-2 imagery. Remote Sens. Environ. 240, 111685.

Bondeau, A., Smith, P.C., Zaehle, S., Schaphoff, S., Lucht, W., Cramer, W., Gerten, D., Lotze-Campen, H., Müller, C., Reichstein, M., Smith, B., 2007. Modelling the role of agriculture for the 20th century global terrestrial carbon balance. Global Change Biol. 13, 679–706.

Boryan, C., Yang, Z., Mueller, R., Craig, M., 2011. Monitoring US agriculture: the US Department of Agriculture, National Agricultural Statistics Service, Cropland Data Layer Program. Geocarto Int. 26 (5), 341–358.

Brown, M.E., de Beurs, K.M., 2008. Evaluation of multi-sensor semi-arid crop season parameters based on NDVI and rainfall. Remote Sens. Environ. 112 (5), 2261–2271.

Brown, M.E., de Beurs, K.M., Marshall, M., 2012. Global phenological response to climate change in crop areas using satellite remote sensing of vegetation, humidity and temperature over 26years. Remote Sens. Environ. 126, 174–183.

Chen, M., Griffis, T.J., Baker, J., Wood, J.D., Xiao, K.e., 2015. Simulating crop phenology in the Community Land Model and its impact on energy and carbon fluxes. J. Geophys. Res. Biogeosci. 120 (2), 310–325.

Cleland, E.E., Chuine, I., Menzel, A., Mooney, H.A., Schwartz, M.D., 2007. Shifting plant phenology in response to global change. Trends Ecol. Evol. 22 (7), 357–365.

De Souza, P.I., Egli, D.B., Bruening, W.P., 1997. Water Stress during Seed Filling and Leaf Senescence in Soybean. Agron. J. 89 (5), 807–812.

Diao, C., 2019. Innovative pheno-network model in estimating crop phenological stages with satellite time series. ISPRS J. Photogramm. Remote Sens. 153, 96–109.

Diao, C., 2020. Remote sensing phenological monitoring framework to characterize corn and soybean physiological growing stages. Remote Sens. Environ. 248, 111960.

Folberth, C., Yang, H., Wang, X., Abbaspour, K.C., 2012. Impact of input data resolution and extent of harvested areas on crop yield estimates in large-scale agricultural modeling for maize in the USA. Ecol. Model. 235-236, 8–18.

Funk, C., Budde, M.E., 2009. Phenologically-tuned MODIS NDVI-based production anomaly estimates for Zimbabwe. Remote Sens. Environ. 113 (1), 115–125.

Gao, F., Anderson, M., Daughtry, C., Johnson, D., 2018. Assessing the Variability of Corn and Soybean Yields in Central Iowa Using High Spatiotemporal Resolution Multi-Satellite Imagery. Remote Sens. 10 (9), 1489.

Gao, F., Anderson, M., Daughtry, C., Karnieli, A., Hively, D., Kustas, W., 2020a. A within-season approach for detecting early growth stages in corn and soybean using high temporal and spatial resolution imagery. Remote Sens. Environ. 242, 111752.

Gao, F., Anderson, M.C., Hively, W.D., 2020b. Detecting Cover Crop End-Of-Season Using VENμS and Sentinel-2 Satellite Imagery. Remote Sens. 12 (21), 3524.

Gao, F., Anderson, M.C., Zhang, X., Yang, Z., Alfieri, J.G., Kustas, W.P., Mueller, R., Johnson, D.M., Prueger, J.H., 2017. Toward mapping crop progress at field scales through fusion of Landsat and MODIS imagery. Remote Sens. Environ. 188, 9–25.

Gao, F., Zhang, X., 2021. Mapping Crop Phenology in Near Real-Time Using Satellite Remote Sensing: Challenges and Opportunities. J. Remote Sens. 2021, 1–14.

Hufkens, K., Melaas, E.K., Mann, M.L., Foster, T., Ceballos, F., Robles, M., Kramer, B., 2019. Monitoring crop phenology using a smartphone based near-surface remote sensing approach. Agric. For. Meteorol. 265, 327–337.

Irwin, S., Good, D., Newton, J., 2015. Early Planting and 2015 Corn Yield Prospects: How Much of an Increase? Farmdoc Daily 5.

Jain, M., Srivastava, A., Balwinder-Singh, Joon, R., McDonald, A., Royal, K., Lisaius, M., Lobell, D., 2016. Mapping Smallholder Wheat Yields and Sowing Dates Using Micro-Satellite Data. Remote Sens. 8 (10), 860.

Johnson, D.M., 2014. An assessment of pre- and within-season remotely sensed variables for forecasting corn and soybean yields in the United States. Remote Sens. Environ. 141, 116–128.

Keating, B.A., Carberry, P.S., Hammer, G.L., Probert, M.E., Robertson, M.J., Holzworth, D., Huth, N.I., Hargreaves, J.N.G., Meinke, H., Hochman, Z., McLean, G., Verburg, K., Snow, V., Dimes, J.P., Silburn, M., Wang, E., Brown, S., Bristow, K.L., Asseng, S., Chapman, S., McCown, R.L., Freebairn, D.M., Smith, C.J., 2003. An overview of APSIM, a model designed for farming systems simulation. Eur. J. Agron. 18 (3-4), 267–288.

Kogan, F., Kussul, N., Adamenko, T., Skakun, S., Kravchenko, O., Kryvobok, O., Shelestov, A., Kolotii, A., Kussul, O., Lavrenyuk, A., 2013. Winter wheat yield forecasting in Ukraine based on Earth observation, meteorological data and biophysical models. Int. J. Appl. Earth Obs. Geoinf. 23, 192–203.

Kucharik, C.J., 2006. A Multidecadal Trend of Earlier Corn Planting in the Central USA. Agron. J. 98 (6), 1544–1550.

Lauer, J., 2012. The effects of drought and poor corn pollination on corn. Field Crops 28, 493–495.

Lauer, J.G., Carter, P.R., Wood, T.M., Diezel, G., Wiersma, D.W., Rand, R.E., Mlynarek, M.J., 1999. Corn Hybrid Response to Planting Date in the Northern Corn Belt. Agron. J. 91 (5), 834–839.

Liao, C., Wang, J., Dong, T., Shang, J., Liu, J., Song, Y., 2019. Using spatio-temporal fusion of Landsat-8 and MODIS data to derive phenology, biomass and yield estimates for corn and soybean. Sci. Total Environ. 650, 1707–1721.

Liu, L., Zhang, X., Yu, Y., Gao, F., Yang, Z., 2018. Real-Time Monitoring of Crop Phenology in the Midwestern United States Using VIIRS Observations. Remote Sens. 10 (10), 1540.

Liu, Z., Hubbard, K.G., Lin, X., Yang, X., 2013. Negative effects of climate warming on maize yield are reversed by the changing of sowing date and cultivar selection in Northeast China. Glob. Change Biol. 19, 3481–3492.

Lokupitiya, E., Denning, S., Paustian, K., Baker, I., Schaefer, K., Verma, S., Meyers, T., Bernacchi, C.J., Suyker, A., Fischer, M., 2009. Incorporation of crop phenology in Simple Biosphere Model (SiBcrop) to improve land-atmosphere carbon exchanges from croplands. Biogeosciences 6 (6), 969–986.

Magney, T.S., Eitel, J.U.H., Huggins, D.R., Vierling, L.A., 2016. Proximal NDVI derived phenology improves in-season predictions of wheat quantity and quality. Agric. For. Meteorol. 217, 46–60.

Manfron, G., Delmotte, S., Busetto, L., Hossard, L., Ranghetti, L., Brivio, P.A., Boschetti, M., 2017. Estimating inter-annual variability in winter wheat sowing dates from satellite time series in Camargue, France. Int. J. Appl. Earth Obs. Geoinf. 57, 190–201.

Mann, M., Kahle, H.-P., Beck, M., Bender, B.J., Spiecker, H., Backofen, R., 2018. MICA: Multiple interval-based curve alignment. SoftwareX 7, 53–58.

Moulin, S., Bondeau, A., Delecolle, R., 1998. Combining agricultural crop models and satellite observations: From field to regional scales. Int. J. Remote Sens. 19 (6), 1021–1036.

Müller, C., Elliott, J., Kelly, D., Arneth, A., Balkovic, J., Ciais, P., Deryng, D., Folberth, C., Hoek, S., Izaurralde, R.C., Jones, C.D., Khabarov, N., Lawrence, P., Liu, W., Olin, S., Pugh, T.A.M., Reddy, A., Rosenzweig, C., Ruane, A.C., Sakurai, G., Schmid, E., Skalsky, R., Wang, X., de Wit, A., Yang, H., 2019. The Global Gridded Crop Model Intercomparison phase 1 simulation dataset. Sci. Data 6, 50.

NASS CPR (2020). https://www.nass.usda.gov/Publications/National_Crop_Progress/ (last accessed October 1, 2020).

Nendel, C., Kersebaum, K.C., Mirschel, W., Wenkel, K.O., 2014. Testing farm management options as climate change adaptation strategies using the MONICA model. Eur. J. Agron. 52, 47–56.

Ortiz-Monasterio, J.I., Dhillon, S.S., Fischer, R.A., 1994. Date of sowing effects on grain yield and yield components of irrigated spring wheat cultivars and relationships with radiation and temperature in Ludhiana, India. Field Crops Res. 37, 169–184.

Otegui, M.E., Nicolini, M.G., Ruiz, R.A., Dodds, P.A., 1995. Sowing Date Effects on Grain Yield Components for Different Maize Genotypes. Agron. J. 87 (1), 29–33.

Ren, J., Campbell, J., Shao, Y., 2017. Estimation of SOS and EOS for Midwestern US Corn and Soybean Crops. Remote Sens. 9 (7), 722.

Richardson, A.D., Hufkens, K., Milliman, T., Aubrecht, D.M., Chen, M., Gray, J.M., Johnston, M.R., Keenan, T.F., Klosterman, S.T., Kosmala, M., Melaas, E.K., Friedl, M. A., Frolking, S., 2018. Tracking vegetation phenology across diverse North American biomes using PhenoCam imagery. Sci. Data 5 (1).

Richardson, A.D., Keenan, T.F., Migliavacca, M., Ryu, Y., Sonnentag, O., Toomey, M., 2013. Climate change, phenology, and phenological control of vegetation feedbacks to the climate system. Agric. For. Meteorol. 169, 156–173.

Rosenzweig, C., Jones, J.W., Hatfield, J.L., Ruane, A.C., Boote, K.J., Thorburn, P., Antle, J.M., Nelson, G.C., Porter, C., Janssen, S., Asseng, S., Basso, B., Ewert, F., Wallach, D., Baigorria, G., Winter, J.M., 2013. The Agricultural Model Intercomparison and Improvement Project (AgMIP): Protocols and pilot studies. Agric. For. Meteorol. 170, 166–182.

Sacks, W.J., Deryng, D., Foley, J.A., Ramankutty, N., 2010. Crop planting dates: an analysis of global patterns. Glob. Ecol. Biogeogr. 19, 607–620.

Sadeh, Y., Zhu, X., Chenu, K., Dunkerley, D., 2019. Sowing date detection at the field scale using CubeSats remote sensing. Comput. Electron. Agric. 157, 568–580.

Sakamoto, T., 2018. Refined shape model fitting methods for detecting various types of phenological information on major U.S. crops. ISPRS J. Photogramm. Remote Sens. 138, 176–192.

Sakamoto, T., Gitelson, A.A., Arkebauer, T.J., 2013. MODIS-based corn grain yield estimation model incorporating crop phenology information. Remote Sens. Environ. 131, 215–231.

Sakamoto, T., Wardlow, B.D., Gitelson, A.A., 2011. Detecting Spatiotemporal Changes of Corn Developmental Stages in the U.S. Corn Belt Using MODIS WDRVI Data. IEEE Trans. Geosci. Remote Sens. 49 (6), 1926–1936.

Sakamoto, T., Wardlow, B.D., Gitelson, A.A., Verma, S.B., Suyker, A.E., Arkebauer, T.J., 2010. A Two-Step Filtering approach for detecting maize and soybean phenology with time-series MODIS data. Remote Sens. Environ. 114 (10), 2146–2159.

Sakamoto, T., Yokozawa, M., Toritani, H., Shibayama, M., Ishitsuka, N., Ohno, H., 2005. A crop phenology detection method using time-series MODIS data. Remote Sens. Environ. 96 (3-4), 366–374.

Schaaf, C., Wang, Z., 2015. MCD43A4 MODIS/Terra+ Aqua BRDF/Albedo Nadir BRDF Adjusted RefDaily L3 Global-500m V006 https://doi.org/10.5067/MODIS/MCD43A4.006 (last accessed March 1, 2020). NASA EOSDIS Land Processes DAAC.

Siebert, S., Ewert, F., 2012. Spatio-temporal patterns of phenological development in Germany in relation to temperature and day length. Agric. For. Meteorol. 152, 44–57.

Son, N.-T., Chen, C.-F., Chang, L.-Y., Chen, C.-R., Sobue, S.-I., Minh, V.-Q., Chiang, S.-H., Nguyen, L.-D., Lin, Y.-W., 2016. A logistic-based method for rice monitoring from multitemporal MODIS-Landsat fusion data. Eur. J. Remote Sens. 49 (1), 39–56.

Sun, L., Gao, F., Xie, D., Anderson, M., Chen, R., Yang, Y., Yang, Y., Chen, Z., 2021. Reconstructing daily 30 m NDVI over complex agricultural landscapes using a crop reference curve approach. Remote Sens. Environ. 253, 112156.

Twine, T.E., Kucharik, C.J., Foley, J.A., 2004. Effects of Land Cover Change on the Energy and Water Balance of the Mississippi River Basin. J. Hydrometeorol. 5 (4), 640–655.

Urban, D., Guan, K., Jain, M., 2018. Estimating sowing dates from satellite data over the U.S. Midwest: A comparison of multiple sensors and metrics. Remote Sens. Environ. 211, 400–412.
Viña, A., Gitelson, A.A., Rundquist, D.C., Keydan, G., Leavitt, B., Schepers, J., 2004. Monitoring Maize (Zea mays L.) Phenology with Remote Sensing. Agron. J. 96, 1139–1147.
Waha, K., Müller, C., Bondeau, A., Dietrich, J.P., Kurukulasuriya, P., Heinke, J., Lotze-Campen, H., 2013. Adaptation to climate change through the choice of cropping system and sowing date in sub-Saharan Africa. Global Environ. Change 23 (1), 130–143.
Walthall, C.L., Anderson, C.J., Baumgard, L.H., Takle, E., Wright-Morton, L., 2013. Climate change and agriculture in the United States: Effects and adaptation.
Wan, Z., Zhang, Y., Zhang, Q., Li, Z.-L., 2002. Validation of the land-surface temperature products retrieved from Terra Moderate Resolution Imaging Spectroradiometer data. Remote Sens. Environ. 83 (1-2), 163–180.
Wardlow, B.D., Kastens, J.H., Egbert, S.L., 2006. Using USDA Crop Progress Data for the Evaluation of Greenup Onset Date Calculated from MODIS 250-Meter Data. Photogramm. Eng. Remote Sens. 72 (11), 1225–1234.
White, M.A., De Beurs, K.M., Didan, K., Inouye, D.W., Richardson, A.D., Jensen, O.P., O'Keefe, J., Zhang, G., Nemani, R.R., Van Leeuwen, W.J.D., Brown, J.F., De Wit, A., Schaepman, M., Lin, X., Dettinger, M., Bailey, A.S., Kimball, J., Schwartz, M.D., Baldocchi, D.D., Lee, J.T., Lauenroth, W.K., 2009. Intercomparison, interpretation, and assessment of spring phenology in North America estimated from remote sensing for 1982–2006. Glob. Change Biol. 15, 2335-2359.
White, M.A., Hoffman, F., Hargrove, W.W., Nemani, R.R., 2005. A global framework for monitoring phenological responses to climate change. Geophys. Res. Lett. 32 (4), n/a–n/a.
Xu, X., Conrad, C., Doktor, D., 2017. Optimising Phenological Metrics Extraction for Different Crop Types in Germany Using the Moderate Resolution Imaging Spectrometer (MODIS). Remote Sens. 9 (3), 254.
Xu, X., Riley, W.J., Koven, C.D., Jia, G., Zhang, X., 2020. Earlier leaf-out warms air in the north. Nat. Clim. Change 10 (4), 370–375.
Xue, J., Su, B., 2017. Significant Remote Sensing Vegetation Indices: A Review of Developments and Applications. J. Sens. 2017, 1–17.
Zeng, L., Wardlow, B.D., Wang, R., Shan, J., Tadesse, T., Hayes, M.J., Li, D., 2016. A hybrid approach for detecting corn and soybean phenology with time-series MODIS data. Remote Sens. Environ. 181, 237–250.
Zeng, L., Wardlow, B.D., Xiang, D., Hu, S., Li, D., 2020. A review of vegetation phenological metrics extraction using time-series, multispectral satellite data. Remote Sens. Environ. 237, 111511.
Zhang, X., Friedl, M.A., Schaaf, C.B., 2006. Global vegetation phenology from Moderate Resolution Imaging Spectroradiometer (MODIS): Evaluation of global patterns and comparison with in situ measurements. J. Geophys. Res. Biogeosci. 111 (G4).
Zhang, X., Friedl, M.A., Schaaf, C.B., Strahler, A.H., Hodges, J.C.F., Gao, F., Reed, B.C., Huete, A., 2003. Monitoring vegetation phenology using MODIS. Remote Sens. Environ. 84 (3), 471–475.
Zhang, X., Goldberg, M.D., 2011. Monitoring fall foliage coloration dynamics using time-series satellite data. Remote Sens. Environ. 115 (2), 382–391.
Zhang, X., Wang, J., Henebry, G.M., Gao, F., 2020. Development and evaluation of a new algorithm for detecting 30 m land surface phenology from VIIRS and HLS time series. ISPRS J. Photogramm. Remote Sens. 161, 37–51.